nature catalysis

Article

https://doi.org/10.1038/s41929-023-01063-7

Metabolic engineering of yeast for the production of carbohydrate-derived foods and chemicals from C_{1-3} molecules

Received: 20 January 2023

Accepted: 18 October 2023

Published online: 05 December 2023

Check for updates

Hongting Tang[1,8], Lianghuan Wu[1,8], Shuyuan Guo[1,8], Wenbing Cao[1], Wenhui Ma[1], Xiang Wang[1], Junfeng Shen[1], Menglin Wang[1,2], Qiannan Zhang[1], Mingtao Huang[3], Xiaozhou Luo[1], Jie Zeng[2], Jay D. Keasling[1,4,5,6,7] ✉ & Tao Yu[1] ✉

The increase in population-related and environmental issues has emphasized the need for more efficient and sustainable production strategies for foods and chemicals. Carbohydrates are macronutrients sourced from crops and undergone transformation into various products ranging from foods to chemicals. Continuous efforts have led to the identification of a promising hybrid system that couples the electrochemical reduction of CO_2 to intermediates containing one to three carbons (C_{1-3}) with the transformation of the intermediates using engineered microorganisms into valuable products. Here we use yeast to transform C_{1-3} substrates into glucose and structurally tailored glucose derivatives, such as the sugar alcohol myo-inositol, the amino monosaccharide glucosamine, the disaccharide sucrose and the polysaccharide starch. By metabolic rewiring and mitigation of glucose repression, the titre of glucose and sucrose reached dozens of grams per litre. These results provide directions for microbial sugar-derived foods and chemicals production from renewable reduced CO_2-based feedstocks.

Agriculture provides food and many raw materials for society, but this field is currently facing enormous challenges. The growing world population, expected to reach almost 9–11 billion people by 2050, needs to be supplied with food and other agricultural products. The global demand for food is projected to increase by 70% by 2050 (refs. 1,2). With limited arable land and the growing threat of climate change, it will be nearly impossible for agriculture to meet growing needs without a notable increase in agricultural productivity. Furthermore, the atmospheric CO_2 concentration has increased sharply to 414 ppm in the past 50 years and is still increasing, which may cause catastrophes with long-lasting effects in the future[3,4]. Therefore, we must find an economically viable strategy to fix CO_2 into useful non-food products without the use of

[1]Shenzhen Key Laboratory for the Intelligent Microbial Manufacturing of Medicines, Key Laboratory of Quantitative Synthetic Biology, Center for Synthetic Biochemistry, Shenzhen Institute of Synthetic Biology, Shenzhen Institute of Advanced Technology, Chinese Academy of Sciences, Shenzhen, China. [2]Hefei National Research Center for Physical Sciences at the Microscale, Key Laboratory of Strongly-Coupled Quantum Matter Physics of Chinese Academy of Sciences, Key Laboratory of Surface and Interface Chemistry and Energy Catalysis of Anhui Higher Education Institutes, Department of Chemical Physics, University of Science and Technology of China, Hefei, China. [3]School of Food Science and Engineering, South China University of Technology, Guangzhou, China. [4]Joint BioEnergy Institute, Emeryville, CA, USA. [5]Biological Systems and Engineering Division, Lawrence Berkeley National Laboratory, Berkeley, CA, USA. [6]Department of Chemical and Biomolecular Engineering & Department of Bioengineering, University of California, Berkeley, CA, USA. [7]Novo Nordisk Foundation Center for Biosustainability, Technical University of Denmark, Lyngby, Denmark. [8]These authors contributed equally: Hongting Tang, Lianghuan Wu, Shuyuan Guo. ✉e-mail: keasling@berkeley.edu; tao.yu@siat.ac.cn

https://doi.org/10.1038/s41929-023-01063-7

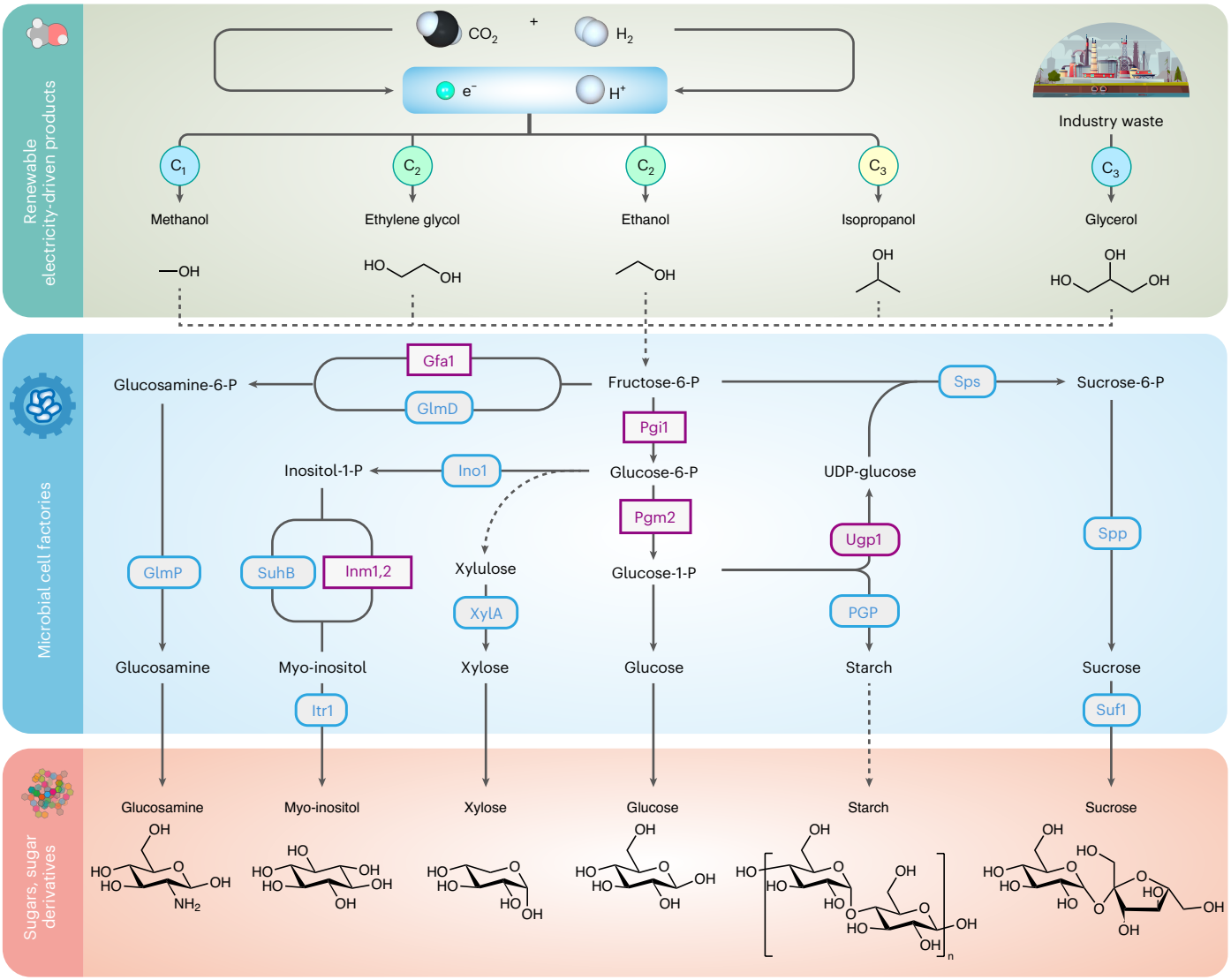

Fig. 1 | Roadmap for production of glucose-derived chemicals from renewable electricity-driven substrates. C_1, C_2 and C_3 chemicals including methanol, ethanol, ethylene glycol, isopropanol and propionate generated by the electrochemical reduction of CO_2 were used as the carbon sources to generate target products. In addition, industry waste glycerol was also used as a carbon source. Yeast cell factories were explored to produce monosaccharide derivatives including glucose, myo-inositol, glucosamine and xylose, and polysaccharide derivatives sucrose and starch. Fructose-6-P, fructose-6-phosphate; Glucose-6-P, glucose-6-phosphate; Glucose-1-P, glucose-1-phosphate; Glucosamine-6-P, glucosamine-6-phosphate; Inositol-1-P, inositol-1-phosphate; Sucrose-6-P, sucrose-6-phosphate; UDP-glucose, uridine diphosphate glucose.

arable land[5]. While natural photosynthesis can reduce atmospheric CO_2, it is important to develop other methods of fixing CO_2 that are faster. Transformation of atmospheric CO_2 by thermochemical[6], electrochemical[7–9], photochemical[10], biochemical approaches[11] and some coupled strategies[12,13] into simple organic compounds with a carbon chain length of $C_{n\leq 3}$ (C_{1-3}) has made great progress in the past few decades. However, these platforms cannot generate complex products or they require complicated in vitro catalytic synthesis. Therefore, combining these platforms with well-known microbial processes that metabolize C_{1-3} substrates into long-chain compounds offers a promising method.

Carbohydrates, such as glucose, sucrose and starch, are some of the most abundant and widely distributed organic substances in nature; furthermore, they are basic components of all organisms. Carbohydrates account for up to 80% of total calorie intake in the human diet[14]. Today, these carbohydrates and their derivatives are the raw materials for a growing diversity of products including food, medicine, commodity and specialty chemicals[15]. Meanwhile, recyclable food technologies are essential for long deep space missions[16]. Recently, the National Aeronautics and Space Administration launched a centennial challenge focused on converting CO_2 into carbohydrates[17]. Several biologic or abiotic approaches have been implemented to complete the conversion of CO_2 to carbohydrates[18–20]. Microbial transformation of C_{1-3} molecules produced by the reduction in CO_2 into carbohydrates has gained widespread interest[19]. This transformation may offer a sustainable alternative to produce these products at lost cost and faster with higher production capacity. The well-studied yeasts *Saccharomyces cerevisiae*[21] and *Pichia pastoris*[22] have been used in the food industry for centuries and are ideally suited for this purpose.

In this Article, we demonstrate a strategy to produce glucose by engineering the microbial transformation of C_{1-3} products (methanol, ethanol and isopropanol) from inorganic CO_2 fixation (Fig. 1). We further expand the products to glucose derivatives, such as sugar alcohols, amino monosaccharides, disaccharides and polysaccharides (Fig. 1). By metabolic rewiring and alleviating glucose repression, the production of glucose and sucrose reached more than 20 g l^{-1}. Glucose-leaking yeast, which lacks glucose activation, could also be an

excellent model system for studying glucose effects rather than using a non-metabolizable glucose analogue[23]. The results demonstrate the technical feasibility of the microbial production of glucose-derived food and chemicals by CO_2 reduction that is powered by renewable energy. With further improvement, this may be an economically viable alternative to agricultural production of these molecules (for more details, see 'Feasibility analysis' in Supplementary Note). In a broader context, the strategy demonstrated here opens the possibility of a renewable energy-driven agriculture and manufacturing industry and could provide a framework for future carbon neutral bioproduction.

Results

Production of glucose from C_{1-3} molecules

Remarkable achievements have been made in the electrochemical reduction of CO_2 into C_{1-3} (refs. 9,24) products (for example, methanol, ethylene, ethanol and isopropanol) using renewable energy. A long-term goal of this field is the direct recycling of CO_2 into higher-carbon products, although, this has rarely been realized[25]. Using model microorganisms to convert the products of inorganic carbon fixation into carbohydrates is a promising way to advance the vision of a circular carbon economy. In our previous work, we described a hybrid electrobiosystem, coupling spatially separate CO_2 electrolysis with yeast fermentation, which efficiently converted CO_2 to acetate by electrolysis, and further to glucose using yeast with an average glucose titre of 1.81 ± 0.14 g l^{-1}. To produce glucose using *S. cerevisiae*, a glucose leaky phenotype was created through the deletion of all known hexokinases—Glk1, Hxk1 and Hxk2. The resulting strain was named LY031 (ref. 20).

To further explore the potential of using other products of electrochemical CO_2 reduction[9], we tested whether *S. cerevisiae* could use the C_1 chemicals methanol and formate, the C_2 chemicals ethylene glycol and oxalic acid, and the C_3 chemicals isopropanol and propionate as carbon sources for cell growth and for the production of valuable products, with glucose serving as an excellent representative compound. In addition, waste glycerol, which has been widely used as an inexpensive carbon source for industrial microbiology, was also utilized. Strain LY031 grew and produced glucose when ethylene glycol, isopropanol, propionate, glycerol or ethanol was used as the sole carbon source (Fig. 2a). This result suggests that cells may have utilization pathways for these chemicals. For example, propionate can be converted to propionyl-CoA by acetyl-CoA synthetase and then enter the methylmalonyl-CoA and 2-methylcitrate pathways[26]. It has been reported that ethylene glycol can be partially oxidized to glyoxylate and further degraded in the glyoxylate degradative pathways[27,28]. Generally, electrochemical reduction of CO_2 produces a variety of compounds, leading to an expensive downstream purification process[29]. Therefore, we hypothesized that we could grow yeast in a mixture of electrochemical reduction products, as microorganisms naturally possess the ability to metabolize multiple carbon sources simultaneously. To demonstrate this concept, we selected ethylene glycol, isopropanol and propionate as constituents of the mixtures due to their ability to be used by *S. cerevisiae*. Different electrocatalysts have been shown to produce a variety of products in various ratios[30,31], and thus different proportions of these compounds were studied. We observed that the ratios of intermediates in the mixtures influenced glucose production and cell growth. Specifically, when ethylene glycol, isopropanol and propionate were present in a proportion of 1:2:3, we achieved a higher glucose titre of 0.72 g l^{-1} and a higher optical density at 600 nm (OD_{600}) of 3.87, compared with an equal ratio (1:1:1) (Supplementary Fig. 1a,b). However, the addition of substrates that cannot be utilized to the mixture did not further increase cell growth and glucose production (Supplementary Fig. 1a).

Except glycerol, the isopropanol culture had the highest OD_{600} (~2.5) and glucose titre (~0.20 g l^{-1}). To further improve isopropanol utilization, several heterologous pathways were tested in *S. cerevisiae*[32,33] (Supplementary Figs. 2 and 4a). We tried the pathway converting isopropanol to acetyl-CoA using alcohol dehydrogenase (Adh), acetone carboxylase complex (Acx), acetoacetyl-CoA synthetase (Aacs) and acetoacetyl-CoA thiolase (Aact)[32]. However, isopropanol utilization was not improved (Supplementary Fig. 4b), even though all heterologous enzymes were confirmed to be expressed on the basis of proteomic analysis (Supplementary Fig. 4c). Therefore, we pursued another strategy that proposed to transform isopropanol into acetate and methanol by enzymatic conversion with Adh, the monooxygenase AcmA and the hydrolase AcmB[33]. The growth of the engineered strains was not improved using isopropanol or acetone as the sole carbon source in different media (Supplementary Fig. 5a,b).

S. cerevisiae has almost no ability to consume formate or methanol (Fig. 2a). Methanol, which is derived from the main greenhouse gases (methane and CO_2), is a potentially renewable C_1 feedstock for biotransformation. Compared with *S. cerevisiae*, the methylotrophic yeast *P. pastoris* has efficient pathways for methanol utilization and can grow using methanol as the sole substrate. However, the engineering of *S. cerevisiae* for methanol utilization performed in previous studies is still in its infancy. Hence, to further verify the generality of the strategy to transform methanol into glucose, we constructed the glucose leaky phenotype in *P. pastoris* by deleting the genes involved in glucose consumption, including all the hexokinase genes *HXK1*, *HXK2*, *GLK1* and *HXK iso2* (encoding hexokinase isoenzyme 2) (Fig. 2b), as was done in *S. cerevisiae*[20]. Strain gsy012 (*glk1Δ*, *hxk1Δ*, *hxk2Δ* and *hxk iso2Δ*) generated glucose and the titre achieved approximately 0.5 g l^{-1} glucose in shake flasks at 96 h (Fig. 2c and Supplementary Fig. 6a) with slight growth defect (Supplementary Fig. 6b). We speculate that the subsequent dephosphorylation of glucose-1-phosphate is also performed properly, presumably by an unknown or non-specific phosphatase in *P. pastoris* (Fig. 2b). Strain gsy012 also showed impaired growth in minimal medium with glucose as the sole carbon source (Fig. 2d and Supplementary Fig. 6c), which further indicated the impaired activity of all hexokinases. To improve the production of glucose by hydrolysing glucose-1-phosphate to glucose, we expressed haloacid dehalogenase-like phosphatase 4, YihX, from *Escherichia coli*[34] (strain gsy013); this resulted in the production of approximately 1.08 g l^{-1} glucose, a nearly 100% improvement compared with gsy012 (Fig. 2c). The volumetric productivity of glucose produced from methanol was determined to be 11.25 mg l^{-1} h^{-1}, corresponding to a glucose yield of 253.62 mg g^{-1} dry cell weight (DCW). Finally, we engineered *P. pastoris* with the isopropanol utilization pathway we engineered into *S. cerevisiae*. Unfortunately, the resulting strains (Supplementary Fig. 3) did not utilize isopropanol or acetone for cell growth any better than the wild-type strain when grown in several media conditions (Supplementary Fig. 7).

Using ethanol as the sole carbon source resulted in high cell growth and glucose production due to the inherent ability of *S. cerevisiae* to grow on ethanol[20]. This result suggests that low glucose production from other low-carbon chemicals may be attributed to weak substrate degradation pathways rather than deficiencies in the glucose synthetic pathway, and optimization of endogenous or heterologous utilization pathways of other various C_{1-3} substrates needs to be further explored. Market analyses indicate ethanol offers greater promise for the future because it possesses a larger market potential[35,36], and thus considerable efforts have been devoted to developing more efficient electrocatalysts for ethanol production, resulting in substantial advancements[37–39]. The Faradaic efficiency (FE) of ethanol of approximately 50% is lower than that of formic acid but higher than methanol and other C_{2+} compounds[40,41]. It is noteworthy that ethanol possesses a combination of advantages over other C_2 compounds such as easier bioavailability, a larger market demand and a high FE. Therefore, ethanol serves as an attractive representative carbon source to expand the repertoire of carbohydrates and overcome potential limitations associated with the inefficient utilization of other substrates.

https://doi.org/10.1038/s41929-023-01063-7

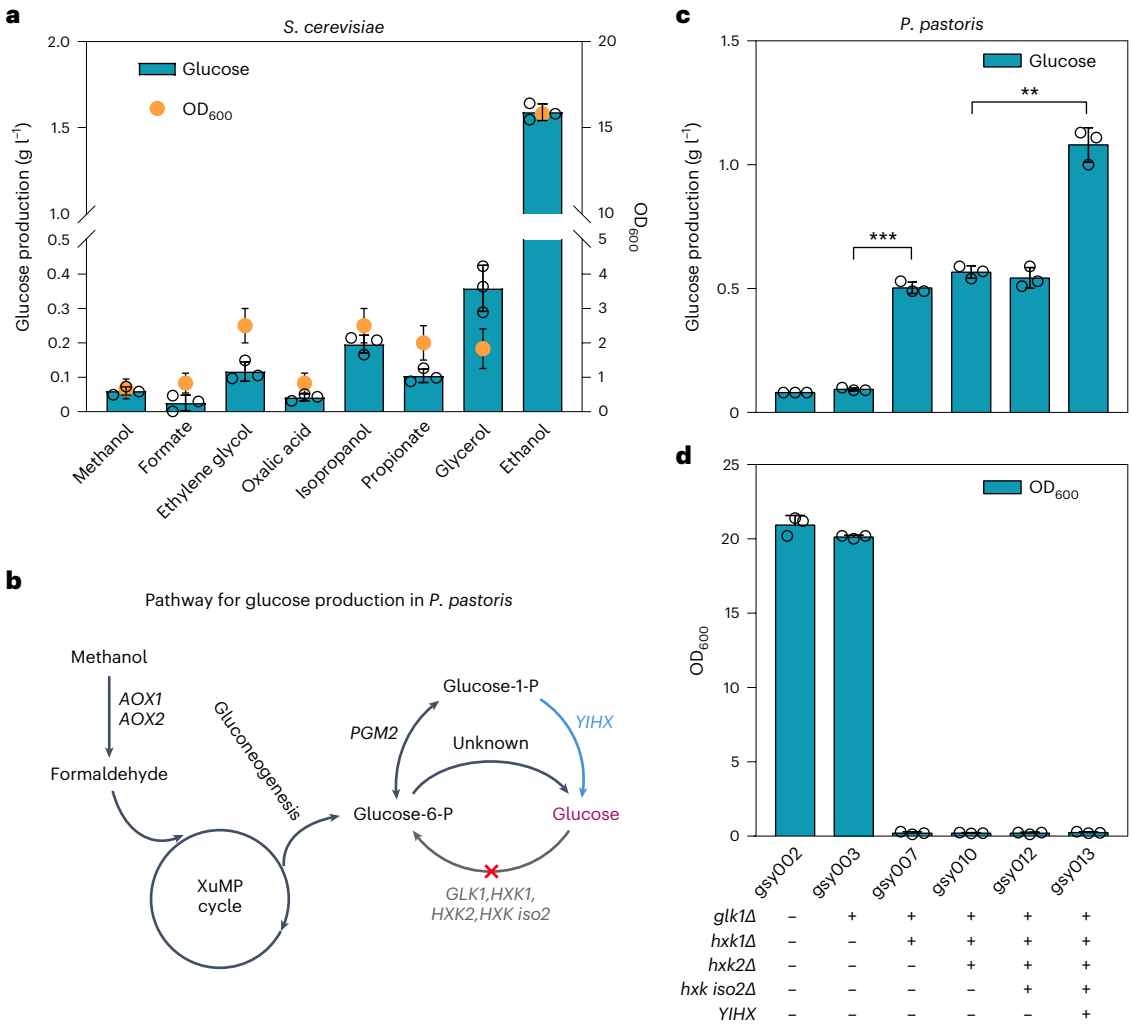

Fig. 2 | Biorefinery of renewable raw materials from C_{1-3} substrates. a, Growth of engineered *S. cerevisiae* and glucose production in different C_{1-3} substrates. *S. cerevisiae* strain LY031 was cultivated in a minimal medium with 10 g l^{-1} yeast extract containing 10 g l^{-1} of methanol, formate, ethanol, ethylene glycol, oxalic acid, isopropanol, propionate or glycerol, respectively. The data of cell growth and glucose production were subtracted from the background in the absence of a carbon source. **b**, Schematic representation of biosynthetic modifications to produce glucose from methanol in *P. pastoris*. Blue arrows, overexpressed genes; grey arrows marked with red X, deleted genes; XuMP, xylulose monophosphate. **c**, Engineered *P. pastoris* produced glucose from methanol at 96 h. **d**, Growth of engineered *P. pastoris* strains in the presence of glucose. Statistical analysis was performed using one-tailed Student's *t*-test (**P<0.01, ***P < 0.001). The P values for the comparisons between group gsy007/gsy003, and group gsy013/gsy010, were 0.00050, and 0.00141, respectively. All data are presented as mean ± s.d. of biological triplicates (n = 3).

Expanding monosaccharide derivatives

To expand the chemical space of glucose derivatives produced by the microbial-electrochemical system, we engineered *S. cerevisiae* to produce other monosaccharides, including hexose derivatives (myo-inositol and glucosamine) and xylose derivatives (xylose and xylitol) using ethanol as a main representative carbon source (Fig. 3a). Myo-inositol is an important compound widely used in the pharmaceutical, cosmetic and food industries[42,43]. Previously, *S. cerevisiae* and *P. pastoris* were engineered to produce myo-inositol; however, glucose was used as the carbon source[44,45]. To efficiently produce myo-inositol from low-carbon substrates, the native inositol-3-phosphate synthase Ino1 was overexpressed and the heterologous *E. coli*'s SuhB that possesses inositol monophosphatase activity was introduced[44]; the native myo-inositol transporter Itr1 was also overexpressed to increase the secretion of myo-inositol into the medium. The optimized strain WX51 (Supplementary Fig. 2) produced 228.71 mg l^{-1} myo-inositol from ethanol in YP medium (Fig. 3b) and 89.58 mg l^{-1} myo-inositol in minimal medium (Supplementary Fig. 8a). In YP medium, the myo-inositol yield and productivity were found to be 47.26 mg g^{-1} DCW and 1.91 mg l^{-1} h^{-1}, respectively. Additionally, we explored the use of isopropanol and glycerol as sole carbon sources for myo-inositol production. Myo-inositol production reached 40.0 mg l^{-1} using glycerol, while no detectable myo-inositol was observed with isopropanol as the carbon source (Supplementary Fig. 8b). For myo-inositol production from methanol, we expressed Ino1p and Irt1 from *P. pastoris* and *E. coli* SuhB in the gsy002 strain (Supplementary Fig. 3). The resulting strain RYT02 produced 129.67 mg l^{-1} of myo-inositol from methanol (Supplementary Fig. 8b).

The amino monosaccharide glucosamine has extensive applications in food, cosmetics and medicines due to its diverse and specific bioactivities[46]. Herein, glucosamine was produced in *S. cerevisiae* from the endogenous precursor glucosamine-6-phosphate by expressing glucosamine-6-phosphate phosphatase GlmP from *Bacteroides thetaiotaomicron*. In addition, glucosamine-6-phosphate deaminase GlmD from *Bacillus subtilis* was also expressed to increase the production of glucosamine-6-phosphate from fructose-6-phosphate. However, no glucosamine was detected when one copy of each of the genes encoding these two enzymes was expressed (Fig. 3c). Thus, we introduced another copy of the two genes and found that the resulting strain CT02

https://doi.org/10.1038/s41929-023-01063-7

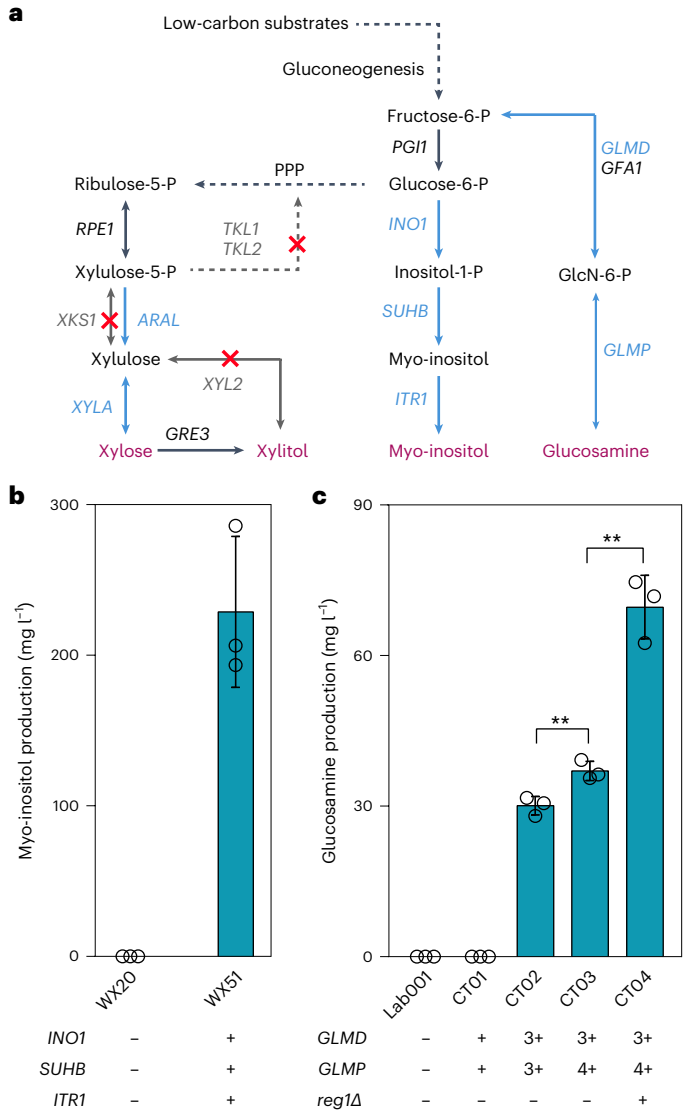

Fig. 3 | Production of monosaccharide derivatives. a, Construction of synthetic pathways for the production of glucosamine, myo-inositol and xylitol. Blue arrows, overexpressed genes; grey arrows marked with red X, deleted genes. **b**, The production of myo-inositol from 120 h fermentation. **c**, The production of glucosamine from 120 h fermentation. 3+, three copies of *GLMD* or *GLMP*, 4+, four copies of *GLMP*. Statistical analysis was performed using one-tailed Student's *t*-test (**$P < 0.01$). The *P* values for the comparisons between group CT03/CT02 and group CT04/CT03 were 0.00525 and 0.00398, respectively. All data are presented as mean ± s.d. of biological triplicates ($n = 3$).

(Supplementary Fig. 2) produced glucosamine at 30.09 mg l^{-1}. Glucosamine production was further improved by increasing the copy number of *GLMP* to a titre of 37.04 mg l^{-1} in YP medium (Fig. 3c) or 19.83 mg l^{-1} in minimal medium with ethanol as the sole carbon source (Supplementary Fig. 9a). When using glycerol as the carbon source, we observed a glucosamine production of 41.69 mg l^{-1}, whereas no detectable glucosamine was observed using isopropanol (Supplementary Fig. 9b). By expressing two copies of *GLMP* and *GLMD*, we achieved a glucosamine production of 29.08 mg l^{-1} from methanol (Supplementary Fig. 9b).

D-Xylose and xylitol are typical five-carbon monosaccharides that are widely used as diabetic sweeteners in foods and beverages[47]; thus, we also tried to produce them from low-carbon sources. Xylose can be synthesized from the endogenous precursor xylulose by the *E. coli* reversible xylose isomerase XylA[48]. Xylitol can be generated from xylose by the native aldose reductase Gre3 and can be cycled into the pentose phosphate pathway (PPP) via xylitol dehydrogenase Xyl2 degradation (Fig. 3a). To reduce the consumption of xylulose-5-phosphate, the transketolases Tkl1 and Tkl2 were deleted (Fig. 3a). Trace amounts (less than 6 mg l^{-1}) of xylose were produced and then consumed later (Supplementary Fig. 10a) when XylA was expressed, and no xylitol was detected. This suggests that the reversibility of XylA, xylulokinase Xks1 and PPP, along with the presence of Gre3 and Xyl2, enables the yeast to consume xylose. To allow xylose conversion into xylitol rather than consumption, we further deleted Xyl2 and Xks1, replacing the latter with the irreversible phosphatase AraL from *Bacillus subtilis*[49] (Fig. 3a). An additional copy of *XYLA* was expressed to strengthen xylose synthesis. The resulting strain ET04 produced 4.30 mg l^{-1} of xylitol from ethanol (Supplementary Fig. 11). Furthermore, by blocking xylose degradation through the deletion of Gre3, we were able to detect 3.52 mg l^{-1} of xylose (Supplementary Fig. 10b).

Expanding oligosaccharide and polysaccharide derivatives

Oligosaccharides and polysaccharides, as well as glucose, are essential agricultural carbohydrates that play a major role in human nutrition. Therefore, we first utilized ethanol to produce these complex carbohydrates. Sucrose is a well-known oligosaccharide and is widely used to produce foods, pharmaceuticals and bulk chemicals. Currently, the main source of sucrose is extraction from sugar cane and sugar beets[50]. The biosynthesis of sucrose in microbial cell factories from low-carbon substrates would be a remarkable achievement; however, this has rarely been reported in yeast. To achieve de novo biosynthesis of sucrose from ethanol in *S. cerevisiae*, two glucose-1-phosphate-based synthetic pathways were studied (Fig. 4a). The biosynthesis of one downstream intermediate, UDP-glucose, was strengthened by overexpression of native UDP-glucose pyrophosphorylase Ugp1, and another ADP-glucose was generated by introduction of a heterologous nonregulated form of ADP-glucose pyrophosphorylase GlgC-TM from *E. coli*[51]. UDP-glucose and ADP-glucose were subsequently catalysed by sucrose-phosphate synthase Sps from *Synechocystis* sp., along with fructose-6-phosphate, to produce sucrose-phosphate. This sucrose-phosphate can be further converted into sucrose by sucrose-phosphate phosphatase (Spp) from *Synechocystis sp*. The sucrose transporter protein Suf1 from *Pisum sativum* is used to transport sucrose out of the cell[52]. To block the sucrose degradation pathway in *S. cerevisiae*, we deleted all the genes encoding sucrose-degrading enzymes, including invertase Suc2; maltases Mal12, Mal22 and Mal32; and isomaltases Ima1, Ima2, Ima3, Ima4 and Ima5 (ref. 50). The resulting strain AT03 (Supplementary Fig. 2) did not grow with sucrose as the sole carbon source, in contrast to the wild-type strain, even though this strain grew normally in the presence of glucose (Supplementary Fig. 12a). Furthermore, integration of *SUF1*, *SPS* and *SPP* into the AT03 genome resulted in strain AT05 that produced 0.82 g l^{-1} sucrose in shake flasks (Fig. 4b). Ugp1 and GlgC-TM were then expressed and the titre of sucrose was increased to 1.17 g l^{-1}, which is a nearly 50% improvement compared with its parent strain; these results illustrated that an increase in the precursors UDP-glucose and ADP-glucose can improve sucrose production. To test whether the activity of Sps and Spp was sufficient for the conversion of the elevated UDP-glucose and ADP-glucose, we added another copy of *SPS* and *SPP* to enhance their expression. However, no remarkable titre improvement was observed (Fig. 4b), indicating that Sps and Spp were not the limiting enzymes in the synthetic pathway. Most of the produced sucrose was secreted into the medium, but approximately 20% was still partially retained in the cells (Fig. 4b), which may be a result of insufficient sucrose transporters. Therefore, one or two more copies of *SUF1* were further overexpressed, but we did not observe any improvement in sucrose secretion (Fig. 4b). AT06 demonstrated a sucrose yield of 351.89 mg g^{-1} DCW, accompanied by a productivity of 9.79 mg l^{-1} h^{-1}. To balance product synthesis with biomass, cell growth was limited by nitrogen supply. There was no notable change in the production capacity of the strains (Supplementary Fig. 12b,c), indicating that the sucrose leakage phenotype is closely

https://doi.org/10.1038/s41929-023-01063-7

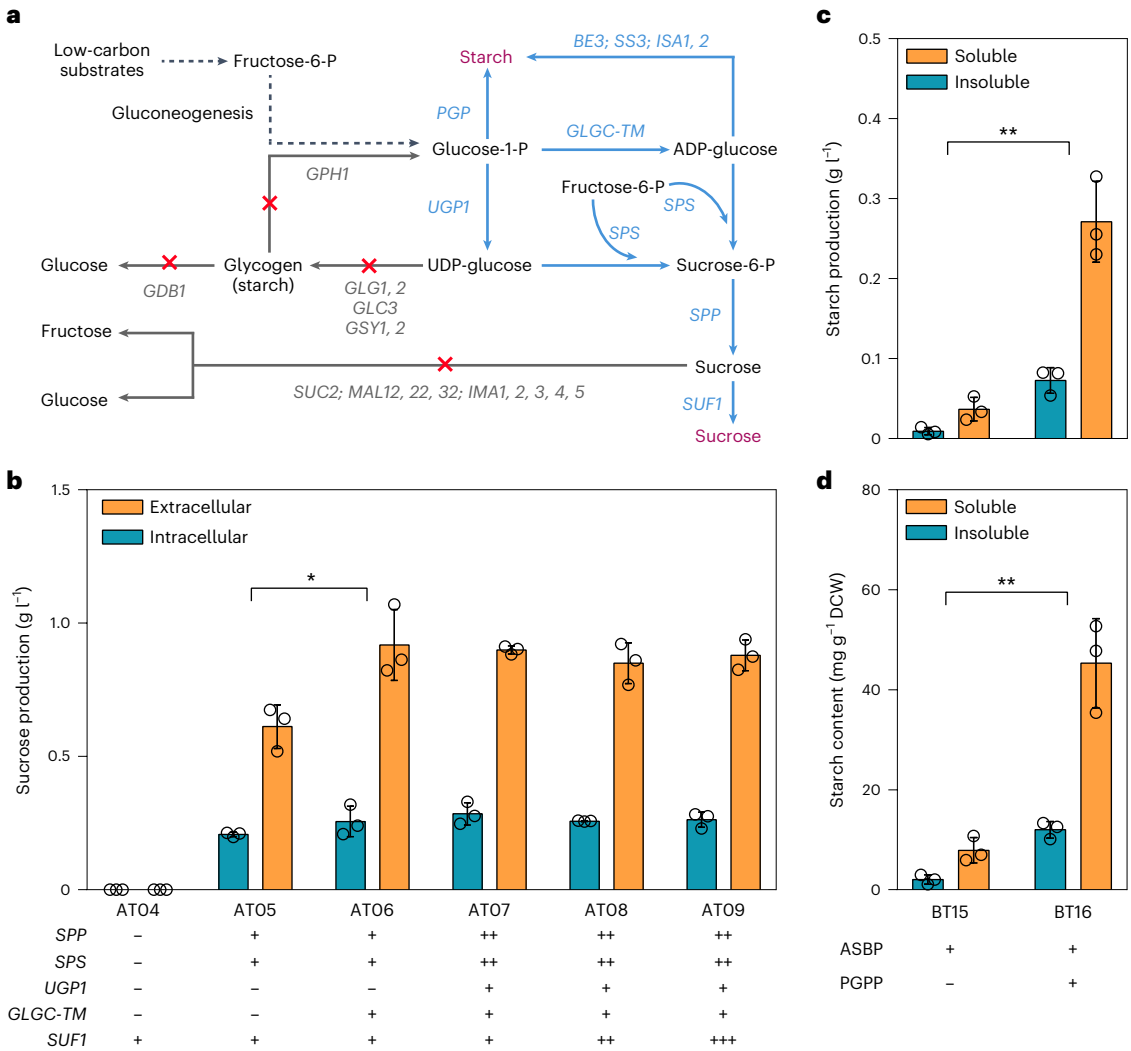

Fig. 4 | Production of oligosaccharide and polysaccharide derivatives. **a**, Biosynthetic pathways for the production of sucrose and starch. Blue arrows, overexpressed genes; grey arrows marked with red X, deleted genes. **b**, Sucrose production in engineered *S. cerevisiae* strains from 120 h fermentation. Orange bars indicate amounts of sucrose secreted into the medium (extracellular), and blue bars indicate amounts of sucrose retained in cells (intracellular). **c**, Starch production in engineered *S. cerevisiae* strains from 120 h fermentation. **d**, Starch content of DCW. Soluble, soluble starch; Insoluble, insoluble starch. Statistical analysis was performed using one-tailed Student's *t*-test (*$P < 0.05$, **$P < 0.01$). The *P* values for the comparisons between group AT06/AT05, group BT16/BT15 for starch production and group BT16/BT15 for starch content were 0.01434, 0.00469 and 0.00471, respectively. All data are presented as mean ± s.d. of biological triplicates ($n = 3$).

related to cell growth. In addition to ethanol, we also used isopropanol and glycerol as sole carbon sources, and the production of sucrose reached 0.38 g l^{-1} and 2.35 g l^{-1}, respectively (Supplementary Fig. 12d). To investigate the possibility of synthesizing sucrose from methanol, we integrated enzymes Sps and Spp, as well as the transporter Suf1, into the *P. pastoris* strain gsy002, which natively cannot utilize sucrose as carbon source. Remarkably, the resulting strain RYT03 produced 0.41 g l^{-1} of sucrose (Supplementary Fig. 12d).

Starches, which are polysaccharides used for excess carbohydrate storage in plants, form the basis of life-sustaining foods and play a primary feedstock role in bioindustries, such as paper manufacturing and biodegradable materials[53,54]. Recently, starch synthesis from CO_2 and H_2 was substantially progressed in a complex cell-free system based on a chemical–biochemical hybrid method[19], although this process consumed a series of expensive purified enzymes. In this study, we tried to achieve the concise microbial production of starch in *S. cerevisiae* from CO_2 via its renewable low-carbon electroderivatives. Previously, the core *Arabidopsis thaliana* starch biosynthesis pathway (ASBP) was introduced in *S. cerevisiae* to study the effect of the biosynthetic enzymes on glucan structure and solubility, and starch was produced in addition to galactose[55]; however, galactose is not a sustainable substrate. In addition, glucose-1-phosphate could also be converted to starch by a one-step reaction catalysed by α-glucan phosphorylase (Pgp)[56,57], herein named the PGP pathway (PGPP). Therefore, two biological pathways, ASBP and PGPP, were synergistically designed to synthesize starch (Fig. 4a). First, we found that the wild-type strain had a high baseline determined by the starch assay kit (Supplementary Fig. 13), and the *Solanum tuberosum* Pgp-expressing strain showed no obvious starch production compared with the wild-type strain (Supplementary Fig. 14a), indicating that endogenous glycogen metabolic pathways may interfere with starch synthesis. To reduce the competitive carbon flux of native glycogen production, we deleted all enzymes including Glg1, Glg2, Glc3, Gsy1 and Gsy2, to block the glycogen biosynthesis pathway. To avoid starch hydrolysis, we also deleted the enzymes Gdb1 and Gph1 (BT13 strain) to abolish the glycogen degradation pathway (Supplementary Fig. 2). To build ASBP, genes encoding ADP-glucose pyrophosphorylase GlgC-TM from *E. coli*, starch synthase SS3, the branching enzyme BE3 and the isoamylases

Isa1 and Isa2 from *A. thaliana* were integrated into the genome of the glycogen-deficient strain, resulting in strain BT12 (Supplementary Fig. 2). This strain produced ~0.20 g l^{-1} starch from glucose, consistent with previous findings[55] (Supplementary Fig. 14b). Pgp was then expressed in strain BT12 by galactose induction using a high-copy plasmid under control of the strong galactose inducible promoter *SkGAL2* from *Saccharomyces kudriavzevii*[58]; the starch titre of this strain reached 0.52 g l^{-1} (Supplementary Fig. 14b), revealing that Pgp expression can improve starch production. Therefore, we integrated *PGP* into the genome of BT12 for stable expression, resulting in strain BT14. Compared to BT12, BT14 had a higher starch production titre of 0.93 g l^{-1} which was approximately a fourfold increase in titre without any growth defects (Supplementary Fig. 14c); this result indicated that PGPP is the major contributor to starch production. Next, we evaluated starch production from ethanol, and the results were similar to those from glucose (Supplementary Fig. 14d). Galactose was required to induce the PGPP because Pgp expression was driven by the *SkGAL2* promoter. To eliminate galactose utilization, the gene encoding galactokinase Gal1, responsible for the conversion of galactose into galactose-1-phosphate, was knocked out in BT12 and BT14, so that galactose would be a gratuitous inducer[59]. The resulting strains BT15 and BT16 produced starch at 46.15 mg l^{-1} and 343.84 mg l^{-1} (Fig. 4c), respectively. The starch content of BT16 reached 57.31 mg g^{-1} DCW (Fig. 4d), which is comparable to the result of starch biosynthesis using galactose as a carbon source[55]. For BT16, the yield of starch produced was 75.30 mg g^{-1} DCW, and the productivity was 2.87 mg l^{-1} h^{-1}. Furthermore, we analysed the starch production of BT16 using isopropanol and glycerol as carbon sources. The production of starch was 26.34 mg l^{-1} and 126.00 mg l^{-1} from isopropanol and glycerol, respectively (Supplementary Fig. 15b). To produce starch from methanol, we disrupted glycogen synthase and glycogenin glucosyltransferase in *P. pastoris* to eliminate glycogen interference (Supplementary Fig. 15a) and introduced ASBP and PGPP to construct strain RYT20 (Supplementary Fig. 3). RYT20 produced 480.08 mg l^{-1} and 117.74 mg l^{-1} of starch from glucose and methanol, respectively (Supplementary Fig. 15a,b).

Metabolic engineering for glucose overproduction

The previous results demonstrated that microbial production of sugar and sugar derivatives from low-carbon sources is doable; thus, we metabolically engineered the microbial platforms for high production to confirm our scheme for synthesizing carbohydrates. In this study, we utilized glucose as the candidate molecule and ethanol as the sole carbon source for this initial work. We first chose to optimize the glucose synthetic pathway by systematically manipulating structural genes in yeast gluconeogenesis metabolism. Many of the reactions in glycolysis and gluconeogenesis are reversible and used in both pathways. The two irreversible reactions transforming pyruvate to phosphoenolpyruvate and fructose-1,6-bisphosphate to fructose-6-phosphate determine the direction of carbon flow[60] (Fig. 5a). To enhance gluconeogenesis and prevent upregulated glycolysis from glucose accumulation, we overexpressed phosphoenolpyruvate carboxykinase Pck1, responsible for transforming oxaloacetate to phosphoenolpyruvate, and deleted pyruvate kinases Pyk1 and Pyk2, enzymes that can convert phosphoenolpyruvate to pyruvate, resulting in a 24.14% improvement in glucose production compared with LY031 (Fig. 5b). The overexpression of fructose-1,6-bisphosphatase Fbp1, which transforms fructose-1,6-bisphosphate to fructose-6-phosphate, and the deletion of phosphofructokinases Pfk1 and Pfk2, which normally convert fructose-6-phosphate to fructose-1,6-bisphosphate, had no notable effect on glucose production (Fig. 5b).

Since the impact of enhancing glucose production by manipulating structural genes is limited, we next sought to develop strategies to increase the flux toward glucose synthesis. Glucose is the preferred carbon source for *S. cerevisiae*. While yeast cells possess the capacity to utilize a variety of carbon sources, it is noteworthy that the presence of glucose inhibits molecular processes associated with the utilization of alternative carbon sources and inhibits the use of the glyoxylate cycle, respiration and gluconeogenesis[23] for cell growth. The repressive impact of glucose on yeast carbon metabolism is orchestrated through a complex interplay of multiple signalling and metabolic interactions (Fig. 5a). The production of glucose or its derivatives, such as glucosamine[61], may generate a glucose-repressive effect, which results in reduced yeast growth and low glucose productivity, thereby inhibiting the use of alternative carbon sources. Thus, there is much interest in rewiring the signalling pathway in microbial platforms to abolish glucose repression. We hypothesized that glucose repression can be alleviated or removed if the regulatory mechanism is properly perturbed and if the regulators that have been reported to regulate glucose repression are manipulated. Snf1 protein kinase signalling is at the heart of glucose repression. The transcriptional repressor Mig1 is the main downstream target of Snf1 phosphorylation (Fig. 5a). It is believed that one of the main functions of Mig1 is to inhibit the transcription of genes involved in gluconeogenesis and respiration when glucose is present[62]. As shown in Fig. 5c, the deletion of Mig1 had almost no effect on glucose production, which suggests the presence and importance of other downstream targets for Snf1. When glucose levels are high, the Snf1 kinase complex loses activity due to self-inhibition resulting from the interaction between its N-terminal catalytic domain and the regulatory domain of the C-terminus. Low concentrations of glucose eliminate this self-inhibition to release Snf1 and allow catalytic activity. In addition, modification of the C-terminal inhibition regulatory subunit from the Snf1 protein also eliminates this self-inhibition. To abolish this self-inhibition, amino acids 381–414 and 381–488 of Snf1 were removed separately[63]. Strain LY037 ($Snf1^{aa381-488\Delta}$) generated glucose at 0.281 g l^{-1} per OD_{600}, which is a 135.78% improvement compared with the 0.119 g l^{-1} per OD_{600} of strain LY039 ($Snf1^{aa381-414\Delta}$) and a 237.58% improvement compared with the 0.083 g l^{-1} per OD_{600} of strain LY031. These results show that relieving glucose repression is conducive to glucose synthesis. However, growth defects limited the application of this strategy (Supplementary Fig. 16a). Activation of Snf1 requires phosphorylation. Phosphatase Glc7 can dephosphorylate Snf1 and is considered the main regulator of Snf1 activity[64]. Reg1 is the regulatory subunit of Glc7 and is involved in the negative regulation of glucose-repressible gene expression[65]. Deletion of Reg1 led to a strain that produced glucose at 0.254 g l^{-1} per OD_{600}, which was 2.05-fold higher than that produced by LY031, and this strain produced glucose at 4.27 g l^{-1} (Fig. 5c and Supplementary Fig. 16a). The yield of glucose from ethanol was 1.25 g g^{-1} DCW, and the productivity was 35.59 mg l^{-1} h^{-1}. In addition, the interaction between the glucose-responsive transcription factor Rgt1 and the Snf1 kinase is critical for hierarchical derepression of the expression of the glucose transporter Hxt; furthermore, this interaction plays an important role in overall glucose repression[66]. To investigate the effect of glucose transport, Rgt1 was deleted to strengthen the inhibition of Hxt expression with or without overexpression of the low-affinity glucose transporter Hxt1 or the high-affinity glucose transporter Hxt4; the cell growth and titre of glucose decreased notably in all engineered strains even though the specific glucose production was similar to that of LY031 (Fig. 5c and Supplementary Fig. 16a). Taken together, these results indicate that efficient glucose export is necessary to alleviate glucose repression and promote cell growth. The Ras–cAMP pathway is one of the main glucose signalling pathways involved in posttranslational regulation by phosphorylation[67]. The G-protein coupled receptor Gpr1 activates the adenylyl cyclase Cyr1 through the GTPase Gpa2 when it responds to external glucose, resulting in a high level of cAMP. Additionally, the GTPases Ras1,2 can also stimulate Cyr1, leading to a rapid increase in cAMP accumulation. The elevated cAMP level causes a dissociation of the catalytic Tpk and regulatory Bcy1 subunits of PKA, leading to the activation of PKA to phosphorylate downstream targets[68,69]. To prevent hyperaccumulation of intracellular cAMP, the phosphodiesterases

https://doi.org/10.1038/s41929-023-01063-7

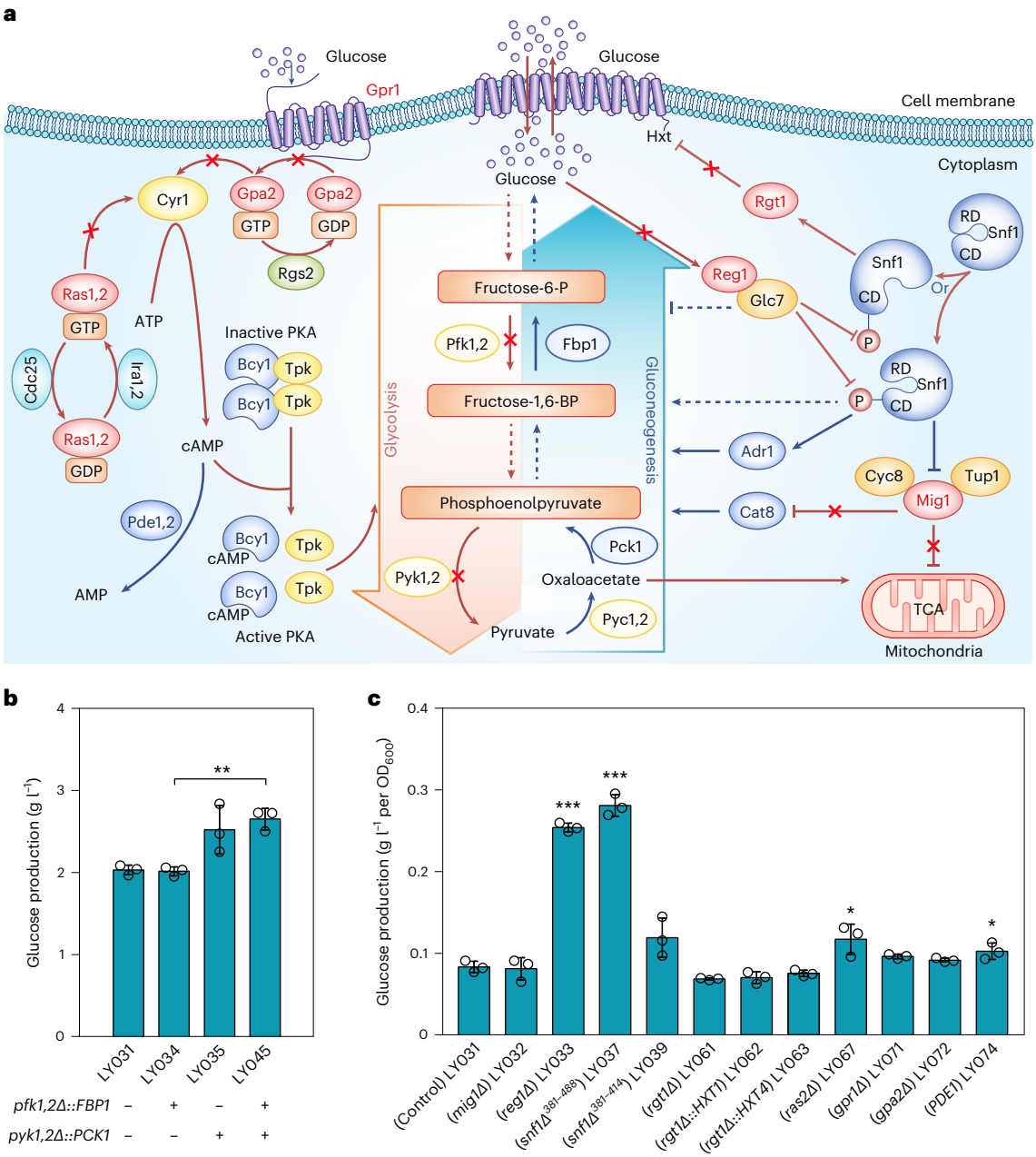

Fig. 5 | Metabolic rewiring of *S. cerevisiae* for glucose overproduction. **a**, One excellent model system for studying glucose effect rather than using non-metabolizable glucose analogue. Biosynthetic modifications to the main glucose repression pathway in *S. cerevisiae* to enhance glucose production. PEP, phosphoenolpyruvate; OAA, oxaloacetate; TCA, tricarboxylic acid; blue arrows, overexpressed genes; grey arrows marked with red X, deleted genes; grey circles, deleted regulators; blue circles, activated regulators. **b**, Manipulating structural genes in yeast gluconeogenesis for glucose production. **c**, Manipulating regulatory genes in glucose repression pathway for glucose production. All engineered strains were cultivated for 120 h, and the samples were used for glucose analysis. Statistical analysis was performed using one-tailed Student's *t*-test (*$P < 0.05$, **$P < 0.01$, ***$P < 0.001$). The *P* values for the comparisons between group LY045/LY034, group LY033/LY031, group LY037/LY031, group LY067/LY031 and group LY074/LY031 were 0.00317 0.00000, 0.00008, 0.03685 and 0.03078, respectively. All data are presented as mean ± s.d. of biological triplicates ($n = 3$).

Pde1 and Pde2 are responsible for regulating cAMP levels by degrading cAMP[70]. Systematic manipulation of this pathway had no notable effect on cell growth and glucose production (Fig. 5c and Supplementary Fig. 16b). In summary, the systematic optimization and redesign of glucose repression was key to improving the production of glucose and its derivatives.

Previously, glucosamine was also shown to have repressive effects similar to glucose[61]. To study whether the positive modification of the glucose-repressive pathway could increase the production of glucosamine, we deleted Reg1, and the glucosamine titre was enhanced to 69.99 mg l^{-1}; however, deletion of Hxk2 had no effect (Fig. 3c). The glucosamine yield was 24.51 mg g^{-1} DCW, and the productivity was 0.58 g l^{-1} h^{-1}. Compared with glucose, the low titre of glucosamine may be caused by the strong inhibition of GlmD and Gfa1 by glucosamine-6-phosphate[71]. To further strengthen gluconeogenesis by alleviating glucose repression for sucrose production, we deleted Hxk2 or Reg1 in strain AT06. However, the *hxk2Δ* strain AT11 produced less sucrose, whereas no detectable change was observed in the *reg1Δ* strain AT10 (Supplementary Fig. 17). AT10 displayed a sucrose yield of 437.81 mg g^{-1} DCW, with a corresponding productivity of 10.98 mg l^{-1} h^{-1}.

https://doi.org/10.1038/s41929-023-01063-7

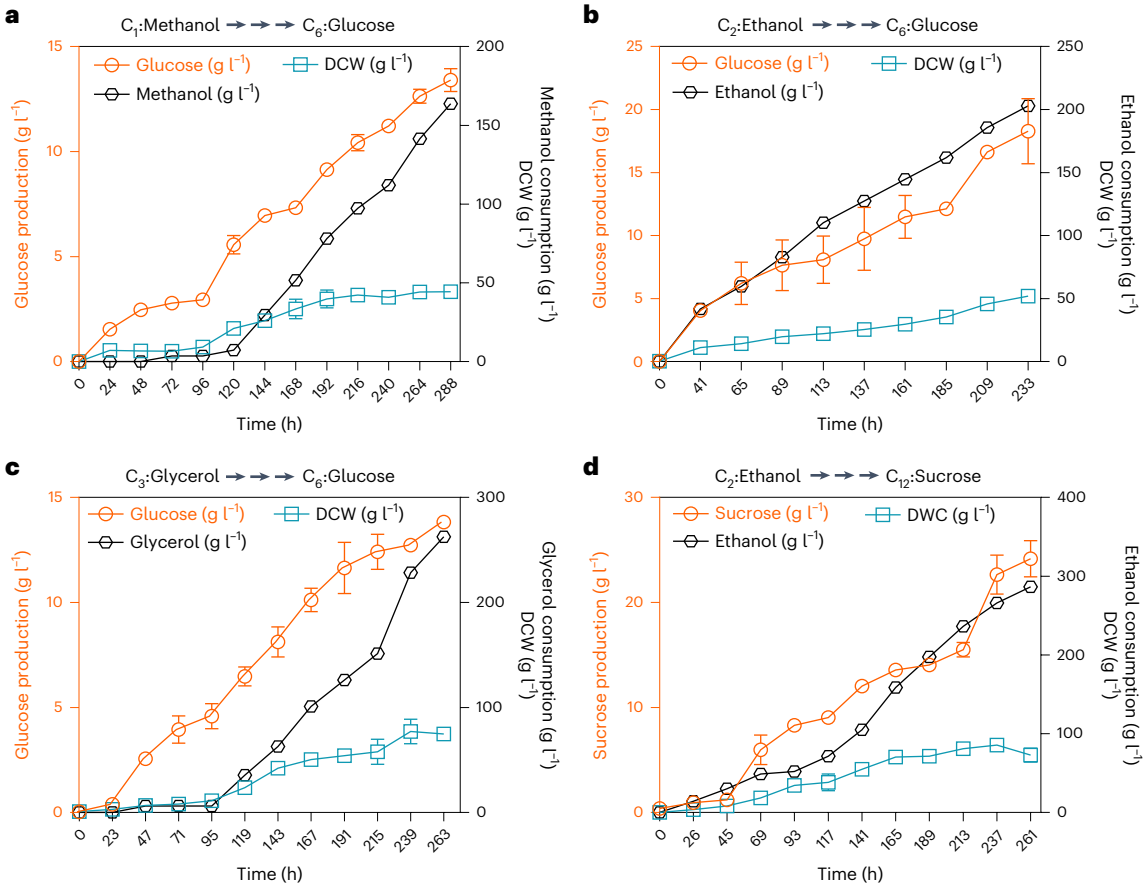

Fig. 6 | Fed-batch fermentation of C_{1-3} substrates by engineered strains. **a**, Glucose production from C_1 substrate methanol by *P. pastoris* gsy013. **b**, Glucose production from C_2 substrate ethanol by *S. cerevisiae* LY033. **c**, Glucose production from C_3 substrate glycerol by *P. pastoris* gsy013. **d**, Sucrose production from ethanol by *S. cerevisiae* AT10. Data of **a**, **c** and **d** are presented as mean ± s.d. of biological triplicates ($n = 3$), and data of **b** are presented as mean ± s.d. of biological duplicates ($n = 2$).

These results suggest that mitigation of glucose repression favours the accumulation of products that are the most important effectors of glucose repression (for example, glucose and glucosamine).

Fed-batch fermentation of the engineered strains

Shake flask evaluations are valuable for strain comparisons; however, they tend to underestimate the strain's potential due to the constraints imposed by limited culture controls, such as O_2 levels and pH. Thus, we characterized the best *P. pastoris* strain (gsy013) and *S. cerevisiae* strains (LY033 and AT10) for glucose and sucrose production from C_{1-3} substrates in fed-batch cultures. First, we evaluated the use of C_1 substrate methanol for glucose production. The gsy013 strain produced 13.41 g l^{-1} glucose and reached a DCW of 44.37 g l^{-1} by consuming 163.65 g methanol at 288 h (Fig. 6a). The yield and productivity of glucose produced from methanol by gsy013 using fed-batch fermentation were 0.30 g g^{-1} DCW and 46.55 mg l^{-1} h^{-1}, respectively, which were higher than those obtained through flask fermentation. Next, LY033 was used to produce glucose from C_2 substrate ethanol, and it produced 18.28 g l^{-1} glucose (Fig. 6b). The final ethanol consumption of 202.97 g and the highest DCW of 52.38 g l^{-1} at 233 h were observed with LY033 (Fig. 6b). The yield of glucose produced from ethanol by LY033 using fed-batch fermentation was determined to be 0.35 g g^{-1} DCW, which represented a 2.5-fold decrease compared with flask fermentation. This decrease suggests that the glucose repression effect, which can be triggered at low glucose concentrations and becomes stronger as the glucose concentration increases[72], may be a rate-limiting step for high glucose production in fed-batch fermentation. The productivity was 78.44 mg l^{-1} h^{-1}, which was higher than flask fermentation. Furthermore, we used gsy013 to produce glucose from C_3 substrate glycerol. The strain gsy013 achieved a glucose production of 13.82 g l^{-1} from 262.48 g of glycerol within 263 h (Fig. 6c). The highest DCW of 74.70 g l^{-1} was observed with the gsy013 strain (Fig. 6c). Finally, we evaluated the production of sucrose as additional product alongside glucose. AT10 consumed 286.48 g ethanol, grew to a DCW of 72.94 g l^{-1} and produced 24.15 g l^{-1} sucrose at 261 h (Fig. 6d). The yield of sucrose produced from ethanol by AT10 using fed-batch fermentation was 332.84 mg g^{-1} DCW, which was comparable to flask fermentation, while the productivity reached 92.54 mg l^{-1} h^{-1}, higher than that of flask fermentation. There was no notable accumulation of byproducts in the fermentation process (Supplementary Figs. 18–21). It is worth noting that glucose repression was partially alleviated by LY033; however, even with this alleviation, the glucose production remained lower compared with that observed with sucrose. This indicates that glucose repression poses challenges for efficient sugar production, and further exploration of glucose repression modulation is necessary to enhance the production. These results indicate that the microbial production of glucose-derived chemicals from $C_n \leqq 3$ has great potential for commercial application.

Discussion

The innovative potential of synthetic biology has led to a surge in interest in using recent advances to address sustainability challenges. One of the most important and attractive challenges is to efficiently assimilate CO_2 in the atmosphere to produce food, fuels and chemicals, which

can greatly compensate for the shortcomings of traditional agricultural and industrial production. In this study, we mainly focused on the microbial conversion of low-carbon chemicals (C_{1-3}), which can be produced from CO_2 using mature electrochemical strategies, into various sugars and their derivatives.

There exist several catalytic routes (electrocatalysis, thermal catalysis or photocatalysis) to produce low-carbon chemicals from CO_2 with negative greenhouse gas emissions[73]. In the future, many more low-carbon chemicals could be produced. Biological metabolism and utilization of these low-carbon chemicals is the main gateway between renewable energy and more complex molecules. In current microbial cell factories, the utilization of sugars extracted from lignocellulosic feedstock remains a challenge. Therefore, expanding the range of substrates that can be used by microbial cell factories is important. Improvement of endogenous catabolic pathways or the introduction of heterologous metabolic pathways to consume low-carbon chemicals from CO_2 fixation is one promising direction. Here, various low-carbon chemicals were tested as the sole carbon source for yeasts, and the results revealed that yeasts can utilize methanol, ethylene glycol, isopropanol and propionate to grow and produce glucose. In addition, the protein content of these engineered strains reached about 50% of the cell dry weight (Supplementary Fig. 22), indicating that single cell protein can be produced accompanied with sugar generation[74]. In the future, *S. cerevisiae* could be further engineered with the integration of functional heterologous pathways for efficient utilization of other chemicals, such as methanol and formate. A better understanding of the principles of low-carbon metabolism and the development of methods to enhance their efficiency is critical to achieving sustainability.

In this study, we detailed the high-titre production of glucose, sucrose, starch and several monosaccharide derivatives, including myo-inositol, and glucosamine. The low xylose yield could be attributed to two potential limiting factors. Xylose synthesis occurs through the PPP. However, in *S. cerevisiae*, the PPP plays only a relatively minor role, with only approximately 2.5% of the glucose being metabolized through the oxidative PPP under standard growth conditions[75]. In contrast, other yeasts exhibit a more balanced contribution from PPP and glycolysis in glucose degradation. Consequently, we believe that the low-carbon source flow flux might be one of the limiting factors for reduced xylose yield in *S. cerevisiae*. Additionally, the reversibility of xylose isomerase[76] and low expression activity in *S. cerevisiae*[77] may serve as another limiting factor for low xylose production. To enhance practical applications, additional efforts in metabolic engineering and enzyme engineering are essential to augment the production yield and rate of these sugars and sugar derivatives from low-carbon chemicals. Glucose production is particularly challenging due to the complex regulation of glucose metabolic pathways. Glucose production was increased substantially by metabolic engineering of the glucose synthetic pathway and the glucose repression pathway, which provided a paradigm for improving other products. For products with a glucose effect, further mitigation of glucose repression is essential. The effect of *reg1Δ* and *snf1Δ*$^{381-488}$ truncation on glucose production is not completely consistent (Fig. 5c and Supplementary Fig. 16a), which implies the existence of a potentially unknown bypass regulation mechanism[23]. The yeast *S. cerevisiae* has long been used as a model for studying glucose repression. To study glucose repression, non-metabolizable glucose analogues have been widely used to mimic glucose[78]. Without glucose phosphorylation/consumption, the glucose leaking yeast could be an excellent model system for studying the glucose effect (Fig. 5a), rather than using non-metabolizable glucose analogues[23]. We achieved the secretion of monosaccharides and the oligosaccharide sucrose but not starch. In the future, engineering yeast to secrete starch would decrease the purification cost and increase its yield; therefore, these methods are worthy of investigation.

In summary, this work demonstrates the practical use of microbial gluconeogenesis metabolism and glucose repression. By combining the overexpression of different terminal conversion enzymes to enhance gluconeogenesis while alleviating glucose repression, the gluconeogenesis metabolism pathway is efficiently diverted to produce glucose-6-phosphate, an important core precursor for the production of sugars and sugar derivatives. The engineering strategy supports the production of these products and shows great potential for commercial production. The production of these sugars and sugar derivatives from low-carbon raw materials demonstrates a necessary and promising step towards realizing a sustainable and more efficient bioprocess than what is available in plants. In a broader context, we believe that the strategy demonstrated here can contribute to the ultimate goal of producing scalable and more efficient sugar-derived foods and renewable chemicals.

Methods

Strains, plasmids and reagents

In this study, all employed plasmids and strains are presented in Supplementary Table 1 and Supplementary Table 2, respectively. 2× Phanta Max Master Mix (catalogue ID: P515) and 2× Phanta Max Master Mix (Dye Plus) (catalogue ID: P525) were purchased from Vazyme Biotech. Gibson assembly kit (catalogue ID: E5510S) and restriction enzyme Dpn1 (catalogue ID: R0176S) were purchased from New England Biolabs. Plasmid miniprep (catalogue ID: DP105), DNA cycle pure kit (catalogue ID: DP204) and DNA gel purification kit (catalogue ID: DP209) were purchased from TIANGEN Biotech. Codon-optimized genes were synthesized and purchased from Sangon Biotech and are listed in Supplementary Table 3. Total starch assay kit (catalogue ID: K-TSTA-100A) was purchased from Megazyme. D-Xylose content assay kit (catalogue ID: BC4395) was purchased from Solarbio Science & Technology. The information for all chemicals, including catalogue ID and sources, is listed in Supplementary Table 4.

Strain cultivation

The plasmids were constructed and propagated using the *E. coli* strain Trans5α. These *E. coli* strains were grown in Luria–Bertani medium, which consisted of 5 g l^{-1} yeast extract, 10 g l^{-1} tryptone and 10 g l^{-1} NaCl. The cultures were maintained at 37 °C and could either include or exclude 100 μg ml^{-1} of ampicillin.

S. cerevisiae strain and *P. pastoris* strain were cultivated in yeast extract peptone medium (YP) consisting of 10 g l^{-1} yeast extract, 20 g l^{-1} peptone and 20 g l^{-1} glucose (YPD), or 20 g l^{-1} ethanol (YPE) or 10 g l^{-1} glycerol, 5 g l^{-1} methanol (YPMG), at 30 °C, 200 rpm for normal cultivation and preparation of competent cells. Strains containing *URA3*-based plasmids were cultivated in synthetic complete (SC) medium without uracil, which contained 8 g l^{-1} SC/-Ura broth and 20 g l^{-1} glucose or 20 g l^{-1} ethanol. The URA3 marker plasmids were removed by using SC + 5-FOA plates, which consisted of 8 g l^{-1} SC/-Ura broth, 100 mg l^{-1} uracil, 0.8 g l^{-1} 5-fluoroorotic acid and 20 g l^{-1} glucose or 20 g l^{-1} ethanol.

Shake flask batch fermentations for production of glucose, glucosamine, myo-inositol, xylose, xylitol and sucrose were carried out in YP or minimal medium containing 7.5 g l^{-1} $(NH_4)_2SO_4$, 14.4 g l^{-1} KH_2PO_4, 0.5 g l^{-1} $MgSO_4{\cdot}7H_2O$, 60 mg l^{-1} uracil, trace metal and vitamin solutions, and supplemented with 20 g l^{-1} ethanol or 20 g l^{-1} methanol or 20 g l^{-1} glycerol or 20 g l^{-1} isopropanol as the carbon sources[79]. Initially, single colonies were inoculated into 2 ml of liquid medium to establish 24 h pre-cultures, and then pre-cultures were inoculated in 100-ml non-baffled flasks with 20 ml liquid medium at an initial OD_{600} of 0.2 for ethanol, 0.5 for glycerol and methanol, and 4 for isopropanol, and cultivated at 200 rpm, 30 °C for 120 h. Shake flask batch fermentations for the production of starch were performed in YPD, YP with 20 g l^{-1} galactose (YPGal), YPE and SC medium without uracil containing 20 g l^{-1} glucose (SCG) or 20 g l^{-1} galactose (SCGal). Twenty-four-hour pre-cultures were inoculated into 100-ml non-baffled flask with 20 ml

YPD, YPE or SCG at an initial OD_{600} of 0.2 and cultivated at 200 rpm, 30 °C for 48 h, and then galactose was added for 120 h. The fermentation was performed for 24 h in YP medium with an initial OD_{600} of 0.5 and a carbon source composition of 20 g l^{-1} methanol and 5 g l^{-1} glucose.

Genetic manipulation

In this study, the background strain for all genetic manipulations in *S. cerevisiae* was Lab001, derived from CEN.PK113-5D. Supplementary Table 5 lists all the primers used in this study. The deletion of genes and the integration of expression cassettes were carried out using the CRISPR–Cas9 system[80]. To identify potential guide RNAs (gRNAs) for specific target genes, we used the Yeastriction webtool (http://yeastriction.tnw.tudelft.nl). The construction of gRNA plasmids was based on the backbone plasmid pLY001 (ref. 20). The fragment containing gRNA sequences and the backbone amplified from pLY001 were assembled by Gibson assembly method to obtain gRNA plasmids[81]. These constructed plasmids were performed sequencing verification. For the amplification of native promoters, genes, homology sequences and terminators, Lab001 genomic DNA served as the template. For codon-optimized genes (Supplementary Table 3), amplification was performed using synthetic plasmids from Sangon Biotech as templates. To assemble the expression cassettes or perform gene deletion repairs, we employed a fusion PCR approach. To begin, primary fragments with overlapping sequences were initially generated via PCR, employing the primers provided in Supplementary Table 5. Following this, the purified PCR products were subjected to a subsequent PCR reaction, omitting the use of any primers, to produce the complete fusion gene. Subsequently, this fusion fragment served as the template for the final PCR step, utilizing primers. The assembled fusion fragments and gRNA plasmids were subsequently utilized for yeast transformation. For the construction of *PGP*-encoding plasmid, the high copy plasmid pJFE3 with a *UAR3* marker was used as the backbone, and the inducible promoter *SkGAL2* and *PGP* were inserted into pJFE3 by Gibson assembly method to form plasmid pTht013.

For *P. pastoris*, we used strain GS115 as the foundational strain for all genetic manipulation. Supplementary Table 5 provides a compressive list of all primers used in this study. To facilitate the deletion of genes and the integration of expression cassettes, we employed the CRISPR–Cas9 system[82]. For the identification of potential gRNAs for targeting gene, we utilized the CRISPRdirect webtool (http://crispr.dbcls.jp). All gRNA plasmids were constructed on the basis of the backbone plasmid BB3cH_pGAP_23*_pLAT1_Cas9 gifted by Professor Gao, and their accuracy was verified by sequencing. To amplify native promoters, genes, homology sequences and terminators, we used GS115 genomic DNA as a template. *E. coli YIHX* encoding haloacid dehalogenase-like phosphatase was synthesized with codon optimization (Supplementary Table 3) and was amplified from the synthetic plasmid from Sangon Biotech as a template. Expression cassette construction and gene deletion repairs were carried out by fusion PCR as described above. DNA transformation was conducted using a condensed electroporation method[83]. The transformed cells were cultivated for 3 days on YPD or YPMG plates containing 100 μg ml^{-1} hygromycin.

Test of various low electro-carbon sources

For the glucose production of *P. pastoris* using methanol as the carbon source, all the strains were pre-cultured in 2 ml YPMG at 30 °C for 24 h. Then, yeast cells were collected by centrifugation at 4,000*g* for 5 min, and inoculated into 20 ml minimal medium containing 20 g l^{-1} methanol and 0.1 g l^{-1} histidine at an initial OD_{600} of 0.5 and cultivated at 200 rpm, 30 °C for 96 h. For the spot assay, *P. pastoris* cells were washed twice in sterile water and serially diluted 10-fold up to 10^{-4}. Five microlitres of each dilution was spotted onto the indicated agar plates (minimal medium containing 0.1 g l^{-1} histidine and 20 g l^{-1} glucose). Plates were incubated at 30 °C for 3–4 days.

For *S. cerevisiae* strain LY031, 10 g l^{-1} of methanol, formate, ethylene glycol, oxalic acid, isopropanol, propionate and glycerol was used as the carbon source, respectively. In addition, 10 g l^{-1} of a mixture with 2.5 g l^{-1} ethylene glycol, 2.5 g l^{-1} oxalic acid, 2.5 g l^{-1} isopropanol and 2.5 g l^{-1} propionate was also used as the carbon source. The pre-cultures of the LY031 strain in YPE were inoculated into 20 ml minimal medium with 10 g l^{-1} yeast extract and various carbon sources at an initial OD_{600} of 0.2 and cultivated at 200 rpm, 30 °C for 120 h. To test the utilization of isopropanol, all engineered strains were cultivated in YP or minimal medium with 20 g l^{-1} isopropanol for 120 h to measure OD_{600}.

Fed-batch fermentation

For the *S. cerevisiae* fed-batch fermentation, single colonies were initially introduced into 2 ml of liquid medium for 24 h pre-cultures, and then pre-cultures were transferred to 250-ml non-baffled flask with 50 ml liquid medium. These strains were grown at 30 °C until OD_{600} of ~3–5. Fed-batch fermentations were performed in 1.3-litre Eppendorf DASGIP Parallel Bioreactors System with an initial volume of 0.5 litres with an initial OD_{600} of 0.3. Before the experiment, the pumps, pH probes and dissolved oxygen probes were calibrated. The bioprocess was monitored and controlled using the DASGIP Control 5.0 System. The temperature, agitation and aeration were kept at 30 °C, 800 rpm and 36 standard litres (sL) h^{-1}, respectively. The pH was automatically maintained at 5.6 through the addition of 4 M NaOH or 2 M HCl, and the acid, alkali and ethanol feed were carried out using DASGIP MP8 multi-pump modules (pump head tubing: 0.5 mm inner diameter, 1.0 mm wall thickness). Gas composition was continuously monitored with a DASGIP Off Gas Analyzer GA4, aeration was controlled and provided by a DASGIP MX4/4 module, and temperature and agitation were maintained by a DASGIP TC4SC4 module. During the initial batch phase of the process, the strains were cultured in a minimal medium containing 5 g l^{-1} $(NH_4)_2SO_4$, 3 g l^{-1} KH_2PO_4, 0.5 g l^{-1} $MgSO_4{\cdot}7H_2O$, 60 mg l^{-1} uracil, trace metal and vitamin solution, 3% v/v ethanol, 1% galactose and 1% yeast extract were supplied additionally for growth. After ethanol and galactose were consumed, ethanol was added and injected through a septum in the bioreactor head plate with a syringe. The salt stock solution containing 50 g l^{-1} $(NH_4)_2SO_4$, 150 g l^{-1} KH_2PO_4, 25 g l^{-1} $MgSO_4{\cdot}7H_2O$, 3 g l^{-1} uracil, trace metal and vitamin solution was also fed according to carbon source addition. DCW analysis was performed by filtrating 3 ml of broth through a pre-weighed 0.22-μm filter membrane. After filtration, the filter was washed three times and then dried in a 65 °C oven for 48 h. Additionally, 1 ml of samples was centrifuged and stored at −20 °C for subsequent high-performance liquid chromatography (HPLC) analysis.

For the *P. pastoris* fed-batch fermentation, the temperature, agitation and aeration were kept at 30 °C, 800 rpm and 36 sL h^{-1}, respectively. The pH was maintained at 5.0 by automatic addition of 4 M NaOH or 2 M HCl. The dissolved oxygen level was set at ≥10%. Medium was utilized as previously[84]. The composition of the medium in the initial batch phase for growth was: 25 g l^{-1} glycerol, 12.6 g l^{-1} $(NH_4)_2HPO_4$, 0.02 g l^{-1} $CaCl_2{\cdot}2H_2O$, 0.5 g l^{-1} $MgSO_4{\cdot}7H_2O$, 0.9 g l^{-1} KCl and 4.35 ml l^{-1} PTM1 trace salts stock solution and 0.01 g l^{-1} histidine. After glycerol was consumed, methanol or glycerol was added by pulse feeding as described above. The salts stock solution containing nitrogen consisted of 50 g $(NH_4)_2SO_4$, 150 g KH_2PO_4, 6.45 g $MgSO_4{\cdot}7H_2O$, 0.35 g $CaCl_2{\cdot}2H_2O$ and 12 ml PTM1 trace salts stock solution per litre methanol or glycerol. Three millilitres of samples were collected every 12 h for DCW analysis as above, and 1 ml of samples were centrifuged and stored at −20 °C for HPLC analysis.

Metabolite extraction and analysis

At the end of shake flask cultivation, all samples were collected and subsequently centrifuged. The supernatant was subjected to membrane filtration (0.22 μm) and frozen at −20 °C for the quantification of extracellular glucose, glucosamine, myo-inositol, xylose, xylitol and

sucrose. Intracellular sucrose was extracted according to the previous study[85]. In brief, the pelleted cells were washed with sterile water and suspended in 1 ml of 80% ethanol (v/v) and then incubated at 65 °C for 4 h, which resulted in nearly complete extraction of compounds with low molecular mass. After centrifugation at 20,000*g* for 5 min, the supernatants were collected and then dried at 40 °C under a steam of N_2. The dried samples were dissolved in ultrapure water and filtered for analysis.

An ultraperformance liquid chromatography–mass spectrometry system equipped with a Jet Stream Technology electrospray ion source (1290-6470, Agilent Technologies) was used for the analysis of glucosamine, and sucrose. Poroshell 120 HILIC-OH5 analytical column (2.1 × 100 mm, 2.7 µm, Agilent Technologies) was used for the separation of glucosamine and sucrose. The program for sample analysis was carried out as follows. Samples were eluted with solvent A (water with 0.1% of formic acid and 5 mM ammonium acetate) and solvent B (80% acetonitrile in water with 0.1% of formic acid and 5 mM ammonium acetate) by the following gradient program at a flow rate of 0.3 ml min^{-1}: 0–3 min, 100% to 95% solvent B; 3–6 min, 95% to 84% solvent B; 6–11 min, 100% solvent B. The injected volume was 2 µl, and the column temperature was set at 30 °C. The flow and temperature of the sheath gas were set at 11 ml min^{-1} and 250 °C, respectively, and the temperature of the nebulizer gas was set at 350 °C. The pressure of the nebulizer was 35 psi. The capillary voltage was set at 3,500 V for the positive ionization mode. Multiple reaction monitoring was selected as scan mode to detect precursor → product ion transitions. Thus, *m*/*z* transitions were 365 → 202.8 (CE: 21) and 365 → 184.7 (CE: 21 V) for sucrose. The glucosamine hydrochlonide *m*/*z* transitions were 202 → 142.8 (CE: 9) and 202 → 111.9 (CE:9 V). Aminex HPX-87H analytical column (7.8 × 300 mm, Bio-Rad) was used for the separation of xylose and xylitol. Samples were eluted with solvent A (water with 0.1% formic acid) using the following gradient program at a flow rate of 0.6 ml min^{-1}. The injected volume was 5 µl, and the column temperature was set at 60 °C. The sheath gas flow rate was configured to 12 ml min^{-1}, and its temperature was maintained at 350 °C. The nebulizer gas temperature was also set at 350 °C. The pressure of the nebulizer was 45 psi, and the capillary voltage was established at 4,000 V for positive ionization mode. Single ion monitoring was selected as scan mode, xylitol (175 *m*/*z*) and xylose (173 *m*/*z*). Xylose concentration was also analysed by D-xylose assay kit according to its instruction.

Starch was quantified by using a total starch assay kit following its instruction. In brief, the washed pellet cells were resuspended in sterile water and transferred into clean tubes along with glass beads (0.5 mm, Biospec), and then mechanically disrupted in a tissue grinding machine (ten times for 30 s each). After centrifugation at 20,000*g* for 5 min, the supernatant containing soluble starch and the cell debris containing insoluble starch were collected, respectively. Two microlitres of undiluted thermostable α-amylase was added to 200 µl of each sample and the mixture was boiled with metal bath at 300 rpm. After 15 min incubation, the temperature was reduced to 50 °C and allowed samples to equilibrate to temperature over 5 min. Next, 0.1 ml of undiluted AMG was added and incubated at 50 °C for 30 min with no further mixing. After incubation, samples were cooled to room temperature and then 10 µl of each sample was added into 3.0 ml of GOPOD reagent for incubation at 50 °C for 20 min. The absorbance of the reaction product was measured at 510 nm.

Glucose, myo-inositol and extracellular metabolites were quantified using the HPLC system (Agilent Technologies 1260 Infinity II SFC). This system is equipped with an Aminex HPX-87H column (Bio-Rad) and a G1362A RID (Agilent Technologies 1260 Infinity II). Pyruvate was detected using the 1260 Infinity II Diode Array Detector WR. The column was eluted with a 5 mM H_2SO_4 at a flow rate of 0.6 ml min^{-1} at a temperature of 50 °C.

Reporting summary

Further information on research design is available in the Nature Portfolio Reporting Summary linked to this article.

Data availability

Source data are provided with this paper.

References

1. Pastor, A. et al. The global nexus of food–trade–water sustaining environmental flows by 2050. *Nat. Sustain.* **2**, 499–507 (2019).
2. Eibl, R. et al. Cellular agriculture: opportunities and challenges. *Annu. Rev. Food Sci.* **12**, 51–73 (2021).
3. Cestellos-Blanco, S. et al. Molecular insights and future frontiers in cell photosensitization for solar-driven CO_2 conversion. *iScience* **24**, 102952 (2021).
4. Sellers, P. et al. Comparison of radiative and physiological effects of doubled atmospheric CO_2 on climate. *Science* **271**, 1402–1406 (1996).
5. Liu, Y. et al. Biofuels for a sustainable future. *Cell* **184**, 1636–1647 (2021).
6. Roy, S., Cherevotan, A. & Peter, S. C. Thermochemical CO_2 hydrogenation to single carbon products: scientific and technological challenges. *ACS Energy Lett.* **3**, 1938–1966 (2018).
7. Ross, M. B. et al. Designing materials for electrochemical carbon dioxide recycling. *Nat. Catal.* **2**, 648–658 (2019).
8. Jia, S. et al. Electrochemical transformation of CO_2 to value-added chemicals and fuels. *CCS Chem.* **4**, 3213–3229 (2022).
9. Grim, R. G. et al. Transforming the carbon economy: challenges and opportunities in the convergence of low-cost electricity and reductive CO_2 utilization. *Energy Environ. Sci.* **13**, 472–494 (2020).
10. Pachaiappan, R. et al. A review of recent progress on photocatalytic carbon dioxide reduction into sustainable energy products using carbon nitride. *Chem. Eng. Res. Des.* **177**, 304–320 (2022).
11. Bierbaumer, S. et al. Enzymatic conversion of CO_2: from natural to artificial utilization. *Chem. Rev.* **123**, 5702–5754 (2023).
12. Yuan, L. et al. Coupling strategy for CO_2 valorization integrated with organic synthesis by heterogeneous photocatalysis. *Angew. Chem. Int. Ed.* **60**, 21150–21172 (2021).
13. Song, X. et al. Towards sustainable CO_2 electrochemical transformation via coupling design strategy. *Mater. Today Sustain.* **19**, 100179 (2022).
14. Davidson, E. A. Carbohydrate. *Encyclopedia Britannica* https://www.britannica.com/science/carbohydrate (2023).
15. Farrán, A. et al. Green solvents in carbohydrate chemistry: from raw materials to fine chemicals. *Chem. Rev.* **115**, 6811–6853 (2015).
16. Martíneza, J. B. G. et al. Chemical synthesis of food from CO_2 for space missions and food resilience. *J. CO2 Util.* **53**, 101726 (2021).
17. Harbaugh, J. NASA awards $750,000 in competition to convert CO_2 into sugar. https://www.nasa.gov/directorates/spacetech/centennial_challenges/75K-awarded-in-competition-to-convert-carbon-dioxide-into-sugar.html (2021).
18. Cestellos-Blanco, S. et al. Toward abiotic sugar synthesis from CO_2 electrolysis. *Joule* **6**, 2304–2323 (2022).
19. Cai, T. et al. Cell-free chemoenzymatic starch synthesis from carbon dioxide. *Science* **373**, 1523–1527 (2021).
20. Zheng, T. et al. Upcycling CO_2 into energy-rich long-chain compounds via electrochemical and metabolic engineering. *Nat. Catal.* **5**, 388–396 (2022).
21. Parapouli, M. et al. *Saccharomyces cerevisiae* and its industrial applications. *AIMS Microbiol* **6**, 1–31 (2020).
22. Spohner, S. C. et al. Expression of enzymes for the usage in food and feed industry with *Pichia pastoris*. *J. Biotechnol.* **202**, 118–134 (2015).
23. Kayikci, Ö. & Nielsen, J. Glucose repression in *Saccharomyces cerevisiae*. *FEMS Yeast Res.* **15**, fov068 (2015).
24. Zhang, B. & Sun, L. Artificial photosynthesis: opportunities and challenges of molecular catalysts. *Chem. Soc. Rev.* **48**, 2216–2264 (2019).

25. Peng, C. et al. Double sulfur vacancies by lithium tuning enhance CO_2 electroreduction to n-propanol. *Nat. Commun.* **12**, 1580 (2021).
26. Pronk, J. T. et al. Propionate metabolism in *Saccharomyces cerevisiae*: implications for the metabolon hypothesis. *Microbiology* **140**, 717–722 (1994).
27. Carnegie, D. & Ramsay, J. A. Anaerobic ethylene glycol degradation by microorganisms in poplar and willow rhizospheres. *Biodegradation* **20**, 551–558 (2009).
28. Pandit, A. V., Harrison, E. & Mahadevan, R. Engineering *Escherichia coli* for the utilization of ethylene glycol. *Microb. Cell. Fact.* **20**, 22 (2021).
29. Snoeckx, R. & Bogaerts, A. Plasma technology—a novel solution for CO_2 conversion? *Chem. Soc. Rev.* **46**, 5805–5863 (2017).
30. Lum, Y. & Ager, J. W. Evidence for product-specific active sites on oxide-derived Cu catalysts for electrochemical CO_2 reduction. *Nat. Catal.* **2**, 86–93 (2019).
31. Lin, Y. et al. Tunable CO_2 electroreduction to ethanol and ethylene with controllable interfacial wettability. *Nat. Commun.* **14**, 3575 (2023).
32. Brown, M. E., Mukhopadhyay, A. & Keasling, J. D. Engineering bacteria to catabolize the carbonaceous component of sarin: teaching *E. coli* to eat isopropanol. *ACS Synth. Biol.* **5**, 1485–1496 (2016).
33. Hausinger, R. P. New insights into acetone metabolism. *J. Bacteriol.* **189**, 671–673 (2007).
34. Pfeiffer, M., Wildberger, P. & Nidetzky, B. Yihx-encoded haloacid dehalogenase-like phosphatase HAD4 from *Escherichia coli* is a specific α-D-glucose 1-phosphate hydrolase useful for substrate-selective sugar phosphate transformations. *J. Mol. Catal. B* **110**, 39–46 (2014).
35. Somoza-Tornos, A. et al. Process modeling, techno-economic assessment, and life cycle assessment of the electrochemical reduction of CO_2: a review. *iScience* **24**, 102813 (2021).
36. Jouny, M. et al. General techno-economic analysis of CO_2 electrolysis systems. *Ind. Eng. Chem. Res.* **57**, 2165–2177 (2018).
37. Li, F. et al. Cooperative CO_2-to-ethanol conversion via enriched intermediates at molecule–metal catalyst interfaces. *Nat. Catal.* **3**, 75–82 (2020).
38. Zhou, Y. et al. Dopant-induced electron localization drives CO_2 reduction to C_2 hydrocarbons. *Nat. Chem.* **10**, 974–980 (2018).
39. Arán-Ais, R. M. et al. The role of in situ generated morphological motifs and Cu(I) species in C_{2+} product selectivity during CO_2 pulsed electroreduction. *Nat. Energy* **5**, 317–325 (2020).
40. Birdja, Y. Y. et al. Advances and challenges in understanding the electrocatalytic conversion of carbon dioxide to fuels. *Nat. Energy* **4**, 732–745 (2019).
41. De Luna, P. et al. What would it take for renewably powered electrosynthesis to displace petrochemical processes? *Science* **364**, eaav3506 (2019).
42. Gonzalez-Uarquin, F., Rodehutscord, M. & Huber, K. Myo-inositol: its metabolism and potential implications for poultry nutrition—a review. *Poult. Sci.* **99**, 893–905 (2020).
43. Li, Y. et al. Production of myo-inositol: recent advance and prospective. *Biotechnol. Appl. Biochem.* **69**, 1101–1111 (2022).
44. Tang, E. et al. Synergetic utilization of glucose and glycerol for efficient myo-inositol biosynthesis. *Biotechnol. Bioeng.* **117**, 1247–1252 (2020).
45. Zhang, Q. et al. Metabolic engineering of *Pichia pastoris* for myo-inositol production by dynamic regulation of central metabolism. *Microb. Cell. Fact.* **21**, 112 (2022).
46. Liu, L. et al. Microbial production of glucosamine and *N*-acetylglucosamine: advances and perspectives. *Appl. Microbiol. Biotechnol.* **97**, 6149–6158 (2013).
47. Shintani, T. Food industrial production of monosaccharides using microbial, enzymatic, and chemical methods. *Fermentation* **5**, 47 (2019).
48. Yin, W. et al. Metabolic engineering of *E. coli* for xylose production from glucose as the sole carbon source. *ACS Synth. Biol.* **10**, 2266–2275 (2021).
49. Godinho, L. M. & de Sá-Nogueira, I. Characterization and regulation of a bacterial sugar phosphatase of the haloalkanoate dehalogenase superfamily, AraL, from *Bacillus subtilis*. *FEBS J.* **278**, 2511–2524 (2011).
50. Marques, W. L. et al. Elimination of sucrose transport and hydrolysis in *Saccharomyces cerevisiae*: a platform strain for engineering sucrose metabolism. *FEMS Yeast Res.* **17**, fox006 (2017).
51. Sakulsingharoj, C. et al. Engineering starch biosynthesis for increasing rice seed weight: the role of the cytoplasmic ADP-glucose pyrophosphorylase. *Plant Sci.* **167**, 1323–1333 (2004).
52. Zhou, Y., Grof, C. P. L. & Patrick, J. W. Proof of concept for a novel functional screening system for plant sucrose effluxers. *J. Microbiol. Methods* **1**, e5 (2014).
53. Jiang, T., Duan, Q., Zhu, J., Liu, H. & Yu, L. Starch-based biodegradable materials: challenges and opportunities. *Ind. Eng. Chem. Res.* **3**, 8–18 (2020).
54. Keeling, P. L. & Myers, A. M. Biochemistry and genetics of starch synthesis. *Annu Rev. Food Sci. Technol.* **1**, 271–303 (2010).
55. Pfister, B. et al. Recreating the synthesis of starch granules in yeast. *eLife* **5**, e15552 (2016).
56. Liu, X. et al. Fusion of cellobiose phosphorylase and potato alpha-glucan phosphorylase facilitates substrate channeling for enzymatic conversion of cellobiose to starch. *Prep. Biochem. Biotechnol.* **52**, 611–617 (2021).
57. You, C. et al. Enzymatic transformation of nonfood biomass to starch. *Proc. Natl Acad. Sci. USA* **110**, 7182–7187 (2013).
58. Peng, B., Wood, R. J., Nielsen, L. K. & Vickers, C. E. An expanded heterologous GAL promoter collection for diauxie-inducible expression in *Saccharomyces cerevisiae*. *ACS Synth. Biol.* **7**, 748–751 (2018).
59. Westfall, P. J. et al. Production of amorphadiene in yeast, and its conversion to dihydroartemisinic acid, precursor to the antimalarial agent artemisinin. *Proc. Natl Acad. Sci. USA* **110**, 7182–7187 (2013).
60. Hers, H. G. & Hue, L. Gluconeogenesis and related aspects of glycolysis. *Annu. Rev. Biochem.* **52**, 617–653 (1983).
61. Flores, C.-L. & Gancedo, C. Construction and characterization of a *Saccharomyces cerevisiae* strain able to grow on glucosamine as sole carbon and nitrogen source. *Sci. Rep.* **8**, 16949 (2018).
62. Santangelo, G. M. Glucose signaling in *Saccharomyces cerevisiae*. *Microbiol. Mol. Biol. Rev.* **70**, 253–282 (2006).
63. Leech, A., Nath, N., McCartney, R. R. & Schmidt, M. C. Isolation of mutations in the catalytic domain of the snf1 kinase that render its activity independent of the snf4 subunit. *Eukaryot. Cell* **2**, 265–273 (2003).
64. Dombek, K. M., Kacherovsky, N. & Young, E. T. The Reg1-interacting proteins, Bmh1, Bmh2, Ssb1, and Ssb2, have roles in maintaining glucose repression in *Saccharomyces cerevisiae*. *J. Biol. Chem.* **279**, 39165–39174 (2004).
65. Rubenstein, E. M. et al. Access denied: Snf1 activation loop phosphorylation is controlled by availability of the phosphorylated threonine 210 to the PP1 phosphatase. *J. Biol. Chem.* **283**, 222–230 (2008).
66. Palomino, A., Herrero, P. & Moreno, F. Tpk3 and Snf1 protein kinases regulate Rgt1 association with *Saccharomyces cerevisiae* HXK2 promoter. *Nucleic Acids Res.* **34**, 1427–1438 (2006).

67. Rolland, F., Winderickx, J. & Thevelein, J. M. Glucose-sensing and -signalling mechanisms in yeast. *FEMS Yeast Res.* **2**, 183–201 (2002).
68. Nishimura, A. et al. The Cdc25/Ras/cAMP-dependent protein kinase A signaling pathway regulates proline utilization in wine yeast *Saccharomyces cerevisiae* under a wine fermentation model. *Biosci. Biotechnol. Biochem.* **86**, 1318–1326 (2022).
69. Wang, Y. et al. Ras and Gpa2 mediate one branch of a redundant glucose signaling pathway in yeast. *PLoS Biol.* **2**, e128 (2004).
70. Ma, P., Wera, S., Van Dijck, P. & Thevelein, J. M. The PDE1-encoded low-affinity phosphodiesterase in the yeast *Saccharomyces cerevisiae* has a specific function in controlling agonist-induced cAMP signaling. *Mol. Cell. Biol.* **10**, 91–104 (1999).
71. Deng, M. D. et al. Metabolic engineering of *Escherichia coli* for industrial production of glucosamine and *N*-acetylglucosamine. *Metab. Eng.* **7**, 201–214 (2005).
72. Yin, Z., Hatton, L. & Brown, A. J. Differential post-transcriptional regulation of yeast mRNAs in response to high and low glucose concentrations. *Mol. Microbiol.* **35**, 553–565 (2000).
73. Wang, F. et al. Technologies and perspectives for achieving carbon neutrality. *Innovation* **2**, 100180 (2021).
74. Molitor, B., Mishra, A. & Angenent, L. T. Power-to-protein: converting renewable electric power and carbon dioxide into single cell protein with a two-stage bioprocess. *Energy Environ. Sci.* **12**, 3515–3521 (2019).
75. Bertels, L. K., Fernández Murillo, L. & Heinisch, J. J. The pentose phosphate pathway in yeasts-more than a poor cousin of glycolysis. *Biomolecules* **11**, 725 (2021).
76. Wong, D. W. S. *Food Enzymes: Structure and Mechanism* Ch. 13 (Springer, 1995).
77. Sarthy, A. V. et al. Expression of the *Escherichia coli* xylose isomerase gene in *Saccharomyces cerevisiae*. *Appl. Environ.* **53**, 1996–2000 (1987).
78. Gancedo, J. M. & Gancedo, C. Catabolite repression mutants of yeast. *FEMS Microbiol. Rev.* **1**, 179–187 (1986).
79. Verduyn, C., Postma, E., Scheffers, W. A. & Van Dijken, J. P. Effect of benzoic acid on metabolic fluxes in yeasts: a continuous-culture study on the regulation of respiration and alcoholic fermentation. *Yeast* **8**, 501–517 (1992).
80. Yu, T. et al. Metabolic engineering of *Saccharomyces cerevisiae* for production of very long chain fatty acid-derived chemicals. *Nat. Commun.* **8**, 15587 (2017).
81. Mans, R. et al. CRISPR/Cas9: a molecular Swiss army knife for simultaneous introduction of multiple genetic modifications in *Saccharomyces cerevisiae*. *FEMS Yeast Res.* **15**, fov004 (2015).
82. Gassler, T., Heistinger, L., Mattanovich, D., Gasser, B. & Prielhofer, R. CRISPR/Cas9-mediated homology-directed genome editing in *Pichia pastoris*. *Methods Mol. Biol.* **1923**, 211–225 (2019).
83. Lin-Cereghino, J. et al. Condensed protocol for competent cell preparation and transformation of the methylotrophic yeast *Pichia pastoris*. *BioTechniques* **38**, 44 (2005). 46, 48.
84. de Lima, P. B. A. et al. Novel homologous lactate transporter improves L-lactic acid production from glycerol in recombinant strains of *Pichia pastoris*. *Microb. Cell Fact.* **15**, 158 (2016).
85. Du, W., Liang, F., Duan, Y., Tan, X. & Lu, X. Exploring the photosynthetic production capacity of sucrose by cyanobacteria. *Metab. Eng.* **19**, 17–25 (2013).

Acknowledgements

This work was financially supported by the National Key Research and Development Program of China (grant no. 2020YFA0907800 to T.Y.), the National Natural Science Foundation of China (grant no. 32071416 to T.Y. and 22308369 to W.C.), the Shenzhen Institute of Synthetic Biology Scientific Research Program (grant no. JCHZ20200003 to T.Y.), Shenzhen Key Laboratory for the Intelligent Microbial Manufacturing of Medicines (grant no. ZDSYS20210623091810032 to T.Y.), Key-Area Research and Development Program of Guangdong Province (grant no. 2022B1111080005 to T.Y.), the Strategic Priority Research Program of the Chinese Academy of Sciences (grant no. XDB0480000 to T.Y.), the National Key Research and Development Program of China (grant no. 2021YFA0911000 to T.Y.), CAS Project for Young Scientists in Basic Research (YSBR-051 to J.Z.), the China Postdoctoral Science Foundation (grant no. 2020M682973 to S.G.) and Guangdong Basic and Applied Basic Research Foundation (grant no. 2020A1515110927 to S.G.). We acknowledge the related fundings supported by China Merchants Research Institute of Advanced Technology Company Limited and China BlueChemical Ltd. We acknowledge the Shenzhen Infrastructure for Synthetic Biology for instrument support and technical assistance with plasmid construction. We thank X. Zhang and L. Xia for critical discussion, and the SIAT Mass Spectrometry Infrastructure for assistance with metabolite analysis.

Author contributions

T.Y. and J.D.K. conceived this study. H.T., L.W. and S.G. designed and performed most of the experiments, analysed the data and drafted the manuscript. W.M., X.W. and J.S. assisted with the experiments and products detection. W.C. assisted with data analysis and interpretation. M.W., Q.Z., X.L. and J.Z. contributed to the manuscript revision. T.Y., J.D.K. and M.H. revised the manuscript. All authors revised and approved the manuscript.

Competing interests

J.D.K. has a financial interest in Amyris, Lygos, Demetrix, Napigen, Maple Bio, Apertor Labs, Zero Acre Farms, Berkeley Yeast and Ansa Biotechnology. X.L. has a financial interest in Demetrix and Synceres. All other authors declare no competing interests.

Additional information

Supplementary information The online version contains supplementary material available at https://doi.org/10.1038/s41929-023-01063-7.

Correspondence and requests for materials should be addressed to Jay D. Keasling or Tao Yu.

Peer review information *Nature Catalysis* thanks Yong-Cheol Park, Rodrigo Ledesma-Amaro and Tianwei Tan for their contribution to the peer review of this work.

nature portfolio

Corresponding author(s): Jay D. Keasling, Tao Yu

Last updated by author(s): September 23, 2023

Reporting Summary

Nature Portfolio wishes to improve the reproducibility of the work that we publish. This form provides structure for consistency and transparency in reporting. For further information on Nature Portfolio policies, see our Editorial Policies and the Editorial Policy Checklist.

Statistics

For all statistical analyses, confirm that the following items are present in the figure legend, table legend, main text, or Methods section.

n/a	Confirmed
☐	☒ The exact sample size (*n*) for each experimental group/condition, given as a discrete number and unit of measurement
☐	☒ A statement on whether measurements were taken from distinct samples or whether the same sample was measured repeatedly
☐	☒ The statistical test(s) used AND whether they are one- or two-sided *Only common tests should be described solely by name; describe more complex techniques in the Methods section.*
☒	☐ A description of all covariates tested
☒	☐ A description of any assumptions or corrections, such as tests of normality and adjustment for multiple comparisons
☐	☒ A full description of the statistical parameters including central tendency (e.g. means) or other basic estimates (e.g. regression coefficient) AND variation (e.g. standard deviation) or associated estimates of uncertainty (e.g. confidence intervals)
☐	☒ For null hypothesis testing, the test statistic (e.g. *F*, *t*, *r*) with confidence intervals, effect sizes, degrees of freedom and *P* value noted *Give P values as exact values whenever suitable.*
☒	☐ For Bayesian analysis, information on the choice of priors and Markov chain Monte Carlo settings
☒	☐ For hierarchical and complex designs, identification of the appropriate level for tests and full reporting of outcomes
☒	☐ Estimates of effect sizes (e.g. Cohen's *d*, Pearson's *r*), indicating how they were calculated

Our web collection on statistics for biologists contains articles on many of the points above.

Software and code

Policy information about availability of computer code

Data collection	Fed-batch fermentations were performed in 1.3 L Eppendorf DASGIP Parallel Bioreactors System. A UPLC-MS system equipped with a Jet Stream Technology electrospray ion source (1290-6470, Agilent Technologies, Santa Clara, CA, USA) was used for the analysis of glucosamine, and sucrose. Poroshell 120 HILIC-OH5 analytical column (2.1*100 mm, 2.7 um, Agilent Technologies, Santa Clara, CA, USA) was used for the separation of glucosamine and sucrose. Aminex HPX-87H analytical column (7.8*300 mm, Biorad, Santa Clara, USA) was used for the separation of xylose and xylitol. Glucose, Myo-inositol and extracellular metabolites were quantified using the HPLC system (Agilent Technologies 1260 Infinity II SFC). This system is equipped with an Aminex HPX-87H column (Bio-Rad) and a G1362A RID (Agilent Technologies 1260 Infinity II).
Data analysis	GraphPad Prism (v 9.0) was used for most data analysis.

For manuscripts utilizing custom algorithms or software that are central to the research but not yet described in published literature, software must be made available to editors and reviewers. We strongly encourage code deposition in a community repository (e.g. GitHub). See the Nature Portfolio guidelines for submitting code & software for further information.

Data

Policy information about availability of data

All manuscripts must include a data availability statement. This statement should provide the following information, where applicable:

- Accession codes, unique identifiers, or web links for publicly available datasets
- A description of any restrictions on data availability
- For clinical datasets or third party data, please ensure that the statement adheres to our policy

All data generated in this study are provided within the paper and its supplementary information files.

Human research participants

Policy information about studies involving human research participants and Sex and Gender in Research.

Reporting on sex and gender	No information was collected
Population characteristics	See above
Recruitment	See above
Ethics oversight	See above

Note that full information on the approval of the study protocol must also be provided in the manuscript.

Field-specific reporting

Please select the one below that is the best fit for your research. If you are not sure, read the appropriate sections before making your selection.

☒ Life sciences ☐ Behavioural & social sciences ☐ Ecological, evolutionary & environmental sciences

For a reference copy of the document with all sections, see nature.com/documents/nr-reporting-summary-flat.pdf

Life sciences study design

All studies must disclose on these points even when the disclosure is negative.

Sample size	Sample size of three (n=3) or more was taken following previous papers in this field.
Data exclusions	The data in Fig.6b are presented as mean ± SD of biological duplicates due to the removal of data from one sample. No data were excluded in the processing of the other figures.
Replication	All data were replicated by triple.
Randomization	The engineered strain colonies were randomly tested.
Blinding	Investigators performing the experiment were blinded to data collection. The researchers performing analytics were blinded for strain information.

Reporting for specific materials, systems and methods

We require information from authors about some types of materials, experimental systems and methods used in many studies. Here, indicate whether each material, system or method listed is relevant to your study. If you are not sure if a list item applies to your research, read the appropriate section before selecting a response.

Materials & experimental systems

n/a	Involved in the study
☒	☐ Antibodies
☒	☐ Eukaryotic cell lines
☒	☐ Palaeontology and archaeology
☒	☐ Animals and other organisms
☒	☐ Clinical data
☒	☐ Dual use research of concern

Methods

n/a	Involved in the study
☒	☐ ChIP-seq
☒	☐ Flow cytometry
☒	☐ MRI-based neuroimaging